Journal of Hazardous Materials 420 (2021) 126569

Contents lists available at ScienceDirect

Journal of Hazardous Materials

journal homepage: www.elsevier.com/locate/jhazmat

Review

Application of layered double hydroxide-biochar composites in wastewater treatment: Recent trends, modification strategies, and outlook

Qianzhen Fang [a,b], Shujing Ye [a,b], Hailan Yang [a,b], Kaihua Yang [a,b], Junwu Zhou [a,b], Yue Gao [a,b], Qinyi Lin [a,b], Xiaofei Tan [a,b,*], Zhongzhu Yang [a,b,*]

[a] College of Environmental Science and Engineering, Hunan University, Changsha 410082, PR China
[b] Key Laboratory of Environmental Biology and Pollution Control (Hunan University), Ministry of Education, Changsha 410082, PR China

ARTICLE INFO

Editor: Dr. H. Artuto

Keywords:
Biochar
Layered double hydroxides
Composite synthesis
Adsorption
Catalysis
Improvement measures

ABSTRACT

In recent years, layered double hydroxide-biochar (LDH-BC) composites as adsorbents and catalysts for contaminants removal (inorganic anions, heavy metals, and organics) have received increasing attention and became a new research point. It is because of the good chemical stability, abundant surface functional groups, excellent anion exchange ability, and good electronic properties of LDH-BC composites. Hence, we offer an overall review on the developments and processes in the synthesis of LDH-BC composites as adsorbents and catalysts. Special attention is devoted to the strategies for enhancing the properties of LDH-BC composites, including (1) magnetic treatment, (2) acid treatment, (3) alkali treatment, (4) controlling metal ion ratios, (5) LDHs intercalation, and (6) calcination. In addition, further studies are called for LDH-BC composites and potential areas for future application of LDH-BC composites are also proposed.

1. Introduction

Biochar (BC), a carbon-rich porous solid material, is produced by pyrolysis of biomass at certain temperature under oxygen-limited condition (Tan et al., 2015; Huang et al., 2017; Li et al., 2016). The source of BC is abundant, such as municipal solid waste, agricultural residues, and timber (X.F. Tan et al., 2016; X. Tan et al., 2016; Meyer et al., 2011; X.H. Wang and Wang, 2019; M. Wang and Wang, 2019; J. Wang and Wang, 2019; Nguyen et al., 2017; Mukome et al., 2013). BC can be used for carbon sequestration, soil fertility improvement and pollution remediation and so on, due to the properties of high surface area, abundant pore structure, surface functional groups, and stable carbon matrix (J. Li et al., 2016; R. Li et al., 2016; Ahmad et al., 2014; Mukherjee et al., 2011; C. Zhang et al., 2020; M. Zhang et al., 2020; W. Zhang et al., 2020; J. Wang et al., 2019; M. Wang et al., 2019; X.H. Wang et al., 2019; Zhang et al., 2019). Among different applications of BC, wastewater treatment has received wide attention because BC has the potential in removing a wide range of pollutants, such as persistent organic compounds, agrochemicals, pharmaceuticals, heavy metals, and nutrients (Tan et al., 2015; Zhang et al., 2020). It is worth emphasizing that BC is a kind of renewable, low cost and sustainable catalyst and adsorbent in wastewater treatment (Mohan et al., 2014). For instance, as an adsorbent, BC has porous structure similar to activated carbon (AC), which is a commonly employed and efficient adsorbent in the removal of contaminants from wastewater (Tan et al., 2015). In addition to adsorption, the environmental persistent free radicals (EPFRs) of BC can react with O_2 to generate hydroxyl radicals (•OH), and BC can also activate persulfate to produce •OH and sulfate radicals (SO_4•$^-$) due to external transition metals and surface functional groups (Lyu et al., 2020; Fang et al., 2015, 2014). And these radicals can degrade organic contaminants efficiently. However, the development of BC also faces some problems. For example, pristine BC has the limitation of adsorption capacity to oxyanions (e.g., phosphate) in wastewater treatment (Wan et al., 2017) and the limitation of dispersity in solution. Hence, the modification and functionalization of pristine BC into the advanced composite with novel structure and surface properties is imperative to expand its applications (H. Zhang et al., 2018; L. Zhang et al., 2018).

Layered double hydroxides (LDHs) are regarded as a group of multi-

Abbreviations: BC, Biochar; MBC, Magnetic biochar; LDH, Layered double hydroxide; LDHs, Layered double hydroxides; CLDH, Calcined layered double hydroxide; LDO, Layered double oxide; LDOs, Layered double oxides; PMS, Peroxymonosulfate; OCS, Oil-tea camellia shell; RHA, Rice husk ash; EDTA, Ethylenediaminetetraacetic acid; MB, Methylene blue; CV, Crystal violet; DS, Diclofenac sodium; AO, Acridine orange.

* Corresponding authors at: College of Environmental Science and Engineering, Hunan University, Changsha 410082, PR China.
E-mail addresses: tanxf@hnu.edu.cn (X. Tan), yzzhnu@126.com (Z. Yang).

https://doi.org/10.1016/j.jhazmat.2021.126569
Received 27 April 2021; Received in revised form 21 June 2021; Accepted 2 July 2021
Available online 3 July 2021

functional anionic clay. The formula of LDHs is $[M^{2+}_{1-x}M^{3+}_{x}(OH)^{2}]^{x+}(A^{n-})_{x/n}{\cdot}mH_2O$, where M^{2+} is a divalent cation, M^{3+} is a trivalent cation, A^{n-} is an interlayer anion and x is the molar ratio of $M^{3+}/(M^{2+}+M^{3+})$, and the layer charge is depended on the M^{2+}/M^{3+}ratio (X.F. Tan et al., 2016; X. Tan et al., 2016; X. Yang et al., 2016; Z. Yang et al., 2016; Jing et al., 2020; Zhang et al., 2016; Wang et al., 2018; K. Yang et al., 2021). LDHs have wide applications in wastewater treatment (Ashekuzzaman and Jiang, 2014; T. Zhang et al., 2017; B. Zhang et al., 2017). Because of the properties of a layered structure, high porosity, high surface area and interlayer anion mobility (X. Yang et al., 2016; Z. Yang et al., 2016), LDHs show great potential in the field of advanced oxidation processes (AOPs) (Yang et al., 2020). Moreover, LDHs are also a kind of excellent and widely used adsorbent in wastewater treatment, which can be used for the removal of various contaminants (e.g., nitrate, phosphate, radionuclides, heavy metals, and organic pollutants) (Zhao et al., 2011; Goh et al., 2008; X. Li et al., 2020; S.B. Li et al., 2020; Ai et al., 2011; C. Shan et al., 2014; R.-R. Shan et al., 2014; Li et al., 2021). However, the development of LDHs is hindered by the problem of tight stacking and high leaching rate during reaction process, which limit the applications as adsorbent and catalyst for removal of contaminants. Therefore, how to improve the deficiencies of LDHs is critical to its development and expansion. According to the reported studies, the environmental application of LDHs will be generally more effective provided that they are dispersed on a matrix which is inexpensive, environmentally recalcitrant, and has additional potential environmental benefits (Wang et al., 2016a). Combined with the above-mentioned properties, BC is a kind of material that meets these requirements.

BC can serve as an effective matrix which provides a large reactive area for effective modification of LDHs and reduces the aggregation of LDHs (X.F. Tan et al., 2016; X. Tan et al., 2016; Zhang et al., 2014; Huang et al., 2019). On the other hand, the sorption efficiency of BC for oxyanions is improved by loaded LDHs due to its interlayer anion mobility and surface complexation (Yang et al., 2019). Besides, the number of surface functional groups on BC also increases, compared with pristine BC. And these surface functional groups may transfer electrons to dissolved oxygen, persulfate, and H_2O_2, forming reactive oxygen radicals for degradation of organic pollutants. What's more, the negative charge features of BC may strengthen the interaction with LDHs nanoparticles, resulting in good chemical stability of LDH-BC composites (H. Zhang et al., 2018; L. Zhang et al., 2018). Therefore, the combination of LDHs with BC is a win-win strategy for both LDHs and BC, in terms of improvement of properties.

Many studies had been reported on the applications of LDH-BC composites in wastewater treatment. However, to our best of knowledge, only a few reviews have summarized the applications of LDH-BC composites, and these reviews are mainly focused on the application of LDH-BC composites in adsorption of pollutants (Vithanage et al., 2020; dos Santos et al., 2021; Zubair et al., 2021a). Therefore, this review comprehensively introduces the applications of this material, including synthesis methods, adsorption, catalysis, and modification strategies. Special attention is devoted to the strategies for enhancing the properties of LDH-BC composites. Although the application of LDH-BC composites in catalysis is not wide enough, based on the excellent catalytic performance of LDHs, we speculate that LDH-BC composites have great potential in catalysis. We elaborate the catalytic mechanisms of LDH-BC composites in detail and provide the reference for future research. At the same time, this review is focused on the modification strategies, and we will explain the specific measures from the perspectives of BC and LDHs based on the existing research to provide ideas for further improving the applications of LDH-BC composites in wastewater treatment.

2. Synthesis methods

At present, there are many methods synthesizing LDH-BC composites. By comparing the specific operations in each experiment, we divide the main synthesis methods into hydrothermal method and co-precipitation method, and the latter can be further divided into post-pyrolysis method and pre-pyrolysis method. Besides, we summarize the main synthetic methods, explain the role of each step from the perspective of operational significance, summarize the general rules, and compare the advantages and disadvantages of different methods to lay the foundation for future research.

2.1. Co-precipitation

2.1.1. Post-pyrolysis method

Post-pyrolysis method was also called the liquid-phase deposition method. By comparing literatures, it could be found that this method was referenced from the synthesis of linear low-density polyethylene (LLDPE)/Zn-Al LDH-exfoliated nanocomposites (Zhang et al., 2013; Chen and Qu, 2004). In general, the main steps of this method were as follows (Fig. 1a). Firstly, after the physical process washing, smashing, and sieving of biomass, the biomass was converted into BC through pyrolysis in a furnace under N_2 flow conditions, and the range of dry-pyrolysis temperature was mainly from 300 °C to 700 °C (Table 1). It needed to be emphasized that the dry-pyrolysis temperature had a great influence on the properties of BC. With the increase of dry-pyrolysis temperature, the production rate decreased but the specifical surface area, carbon content, and thermal stability increased (Sun et al., 2014). The pH values of the regular dry-pyrolysis BC suspensions ranged from 7.1 to 9.2, so most dry-pyrolysis BC suspensions are alkaline, and the surface was positively charged, which might facilitate the integration of BC and LDHs (Sun et al., 2014; Lehmann et al., 2011). Secondly, the pH value of aqueous solution containing mixed metal solution and BC was adjusted to approximately 10, which was the core of coprecipitation. In more details, the BC was firstly suspended in deionized water, and then, the metal solution and the alkaline solution were dripped simultaneously. The pH value of slurry was adjusted by controlling the droplet acceleration of two solutions. pH control was treated as the most important step in this process. The formed structure of LDHs might be not complete in lower pH value, and the formed LDHs might re-dissolve in higher pH value. Therefore, it was found that the synthesis of LDHs was the most beneficial when pH was controlled at about 10 (J. Li et al., 2016; R. Li et al., 2016; Zhang et al., 2013; Lee et al., 2019; Meili et al., 2019). In this step, LDHs were synthesized and attached to the BC surface. Thirdly, the obtained slurry needed to be aged. The aim of this step was to make the structure and chemical properties of the initial LDHs more stable and prevented it from being destroyed by the slight interference of external forces. The experimental conditions used in this aging phase were shown in Table 1. In general, the experimental conditions for this aging phase were various, which could be divided into two categories: (1) traditional one that aged in the original reaction vessel; and (2) hydrothermal treatment that needed to be transferred to the reaction kettle (Zhang et al., 2014). It could be found that the temperature was higher about the reaction conditions of the latter, but the reaction time was often shorter, which indicated that the latter might be more efficient.

2.1.2. Pre-pyrolysis method

In addition to post-pyrolysis method, pre-pyrolysis method has also been used to synthesize the composite, which was shown in Fig. 1b. In this method, LDHs pre-coated biomass was firstly synthesized, which was the biggest difference from pre-pyrolysis method. And other processes were like those steps of post-pyrolysis method. After aging, the dried solids (LDH-biomass mixtures) were converted into layered double oxide (LDO)-BC composites, which was a way to improve LDH-BC composites performance (Yang et al., 2020). For example, LDO-BC composites could reconstruct the original structure by adsorbing anions and this might be conducive to the adsorption of anionic pollutants (X.F. Tan et al., 2016; X. Tan et al., 2016; Jiang et al., 2019). Besides, calcination converted the mixed metal hydroxide into the corresponding

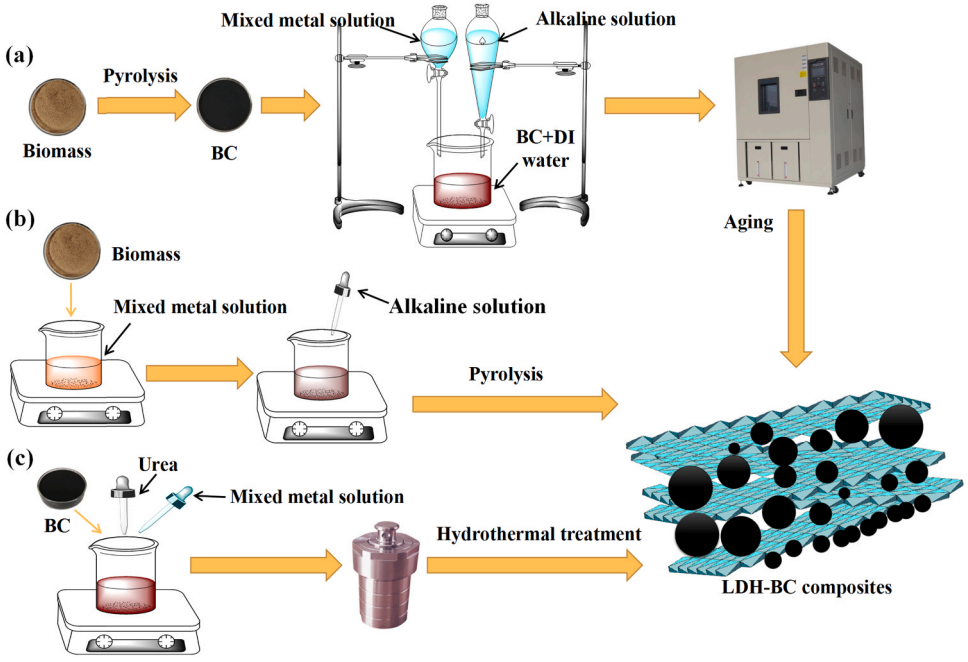

Fig. 1. (a) The schematic diagram of post-pyrolysis method; (b) Pre-pyrolysis method; and (c) Hydrothermal method.

metal oxides mixed with uniformed M^{2+} and M^{3+} distribution with high surface areas, which improved the properties of LDH-BC composites in the photocatalytic application (Zhang et al., 2019).

2.2. Hydrothermal method

In the above synthesis methods, the alkaline solution was used to control the pH value of the reaction system. Urea used as the pH value regulator was one of the most important characteristics of hydrothermal method (Jiang et al., 2019; Wang et al., 2020a, 2020b; Luo et al., 2020; Z. Yang et al., 2021). Besides, urea and alkaline solution had different influences on the structures of LDH-BC composites. In detail, the former could be used to synthetize LDH-BC composites with a regular-shaped (Gholami et al., 2020a). Therefore, we summarized the method on urea as the pH regulator into another method called hydrothermal method or the urea method. The flowchart of the urea method was shown in Fig. 1c. In contrast to other methods, the steps of the urea method were the easiest to operate, which could be divided into two main steps. The first step was to mix BC, metal ion solution and urea solution. The second step was the hydrothermal treatment, which mainly promoted the decomposition of urea and enhances the stability of LDHs in the composite. When ordinary alkaline solution was used to adjust pH, LDHs had been formed quickly and attached to the surface of BC. However, when urea was used to regulate pH, the pH value of the solution changed little due to the slow decomposition rate of urea at room temperature. At this time, the mixture was only the suspension formed by the solution and BC together. Subsequent hydrothermal treatment would provide necessary conditions for the formation of LDH-BC composites. In the hydrothermal treatment process, the decomposition rate of urea was controlled by temperature during heating, which gave the required increases in pH value (Geng et al., 2013), and LDHs gradually grow on the BC matrix. Hence, compared with co-precipitation, LDHs synthesized by urea method had a higher crystallinity and larger average particle size (Geng et al., 2013). As shown in Table 1, in addition to the above three methods, other methods have also been applied, such as the two-step electro-assisted modification method. However, the synthesis methods of LDH-BC composites remained to be developed.

2.3. Advantages and disadvantages of different synthesis methods

The biomass is converted into BC before loading with LDH in post-pyrolysis method and hydrothermal method. And their pyrolysis temperatures are similar in this process (Table 1). However, the most aging temperatures of post-pyrolysis method are lower than 90 °C, which are lower than that of hydrothermal method (>100 °C) (Table 1). This indicates that post-pyrolysis method is more energy-efficient than hydrothermal method. Besides, the reaction processes of post-pyrolysis method are easily controllable than other methods, and post-pyrolysis method is propitious to large-scale production of LDH-BC composites (Zubair et al., 2021a; Bukhtiyarova, 2019). The most common alkaline solution used in post-pyrolysis method is pure NaOH solution or the mixture of Na_2CO_3 and NaOH (Wang et al., 2016a; Meili et al., 2019; Y. Wang et al., 2018; T. Wang et al., 2018; Wang and Wang, 2018; Huang et al., 2019). Urea is the main alkaline solution used in hydrothermal method and can promote formation of LDH with higher crystallinity in comparison with LDH-BC composites obtained by post-pyrolysis method with mixture solution of Na_2CO_3 and NaOH (Luo et al., 2020; Wang et al., 2020b; Bukhtiyarova, 2019; Gholami et al., 2020b). What's more, the particle size distribution of LDH loaded on BC is controllable in hydrothermal method.

Compared with post-pyrolysis method and hydrothermal method, pre-pyrolysis method reduces the number of preparation steps (Lee et al., 2019). Besides, pre-pyrolysis method may enhance the adsorption efficiency of LDH-BC composites. In detail, thermal treatment increases the specific surface area and removes interlayer anions, leading to more binding sites and easier intercalation of anions into interlayer regions (Lee et al., 2019; Cai et al., 2012; Cheng et al., 2010). However, the crystallinity of LDH-BC composites by pre-pyrolysis method is lower than that of post-pyrolysis method and hydrothermal method (Zubair et al., 2021a).

3. Application of LDH-BC composites in wastewater treatment

3.1. Application of LDH-BC composites in adsorption

Through relevant literature currently published, LDH-BC composites were mainly used as adsorbent for the removal of heavy metals (H.

Table 1
Application of LDH-BC composites for water pollution control.

Composites	Biomass	Temperature	Pollutants	Adsorptive capacity (mg/g)	Synthetic methods[a]	Aging condition	References
Mg-Fe LDH/BC	Kiwi branch	500 °C	Cd(II)	25.6	I	3 d, 80 °C	(Tan et al., 2019)
Mg-Fe LDH@BC	Rice straw	600 °C	Cd(II)	126.30	I	24 h, 70 °C	(H. Zhang et al., 2018; L. Zhang et al., 2018)
Mg-Al LDH/BC	Wheat straw	600 °C	Cd(II)	54.14	I	12 h, 80 °C	(Lv et al., 2020)
Mg-Al LDH-EDTA/BC	Bamboo	480 ℃	Cr(VI)	38	II	12 h, 60 °C	(Z. Huang et al., 2019; D. Huang et al., 2019)
Mg-Al LDH/BC	Pinewood	350 ℃	Cr(VI)	330.8	III	10 h, 160 °C	(Wang et al., 2020a)
Mg-Al LDH/BC	PSR[b]	500 ℃	Cr(VI)	No	I	18 h, 60 °C	(M. Li et al., 2019; G.W. Li et al., 2019)
Mn-Al LDH/BC	OCS[b] powder	600 ℃	Cu(II)	74.07	I	1 h, 100 °C	(Y. Wang et al., 2018; C. Wang et al., 2018; T. Wang et al., 2018)
Mg-Fe LDH@BC	Rice straw	600 ℃	Cu(II)	295.80	I	24 h, 70 °C	(H. Zhang et al., 2018; L. Zhang et al., 2018)
Ni-Zn-Fe LDH/BC	Banana peel	600 ℃	Cu(II)	58.48	I	80 °C	(Shafiq et al., 2020)
Mg-Al LDH/BC	corn straw	350 ℃	Cu(II)	75.4	I	12 h, 55 °C	(Peng et al., 2021)
Mg-Al LDH/BC	corn straw	550 ℃	Cu(II)	78.2	I	12 h, 55 °C	(Peng et al., 2021)
Mg-Al LDH/BC	corn straw	750 ℃	Cu(II)	92.5	I	12 h, 55 °C	(Peng et al., 2021)
Mg-Al LDH/BC	corn straw	950 ℃	Cu(II)	94.7	I	12 h, 55 °C	(Peng et al., 2021)
Mg-Fe LDH@BC	Rice straw	600 ℃	Ni(II)	75.59	I	24 h, 70 °C	(H. Zhang et al., 2018; L. Zhang et al., 2018)
Mg-Al LDH/Hydrochar	Sludge	120 ℃	Pb(II)	62.441	III	24 h, 120 °C	(Luo et al., 2020)
Mg-Fe LDH/BC	OCS[b] powder	600 ℃	Pb(II)	476.25	I	6 h, 120 ℃	(Jia et al., 2019)
Mg-Al LDH/BC	Pinewood	350 ℃	Pb(II)	591.2	III	10 h, 160 °C	(Wang et al., 2020a)
Mg-Fe LDH@BC	Rice straw	600 ℃	Pb(II)	1264.10	I	24 h, 70 °C	(H. Zhang et al., 2018; L. Zhang et al., 2018)
Zn-Fe LDH/BC	Orange peel	800 ℃	Pb(II)	69	I	15 h, 70 °C	(Shafiq et al., 2021)
Mg-Fe LDH@BC	Rice straw	600 ℃	Zn(II)	141.70	I	24 h, 70 °C	(H. Zhang et al., 2018; L. Zhang et al., 2018)
Ca-Al LDH/BC	SC[b]	700 ℃	Eu(III)	120.482	I	No	(X. Li et al., 2020; S.B. Li et al., 2020)
Mg-Al LDH/PBC[b]	bamboo	700 ℃	U(VI)	274.15	I	8 h, 90 ℃	(Lyu et al., 2021)
Mg-Al LDH/BC	PSR[b]	500 ℃	SZ[b]	Above 97%	I	18 h, 60 °C	(M. Li et al., 2019; G.W. Li et al., 2019)
Mg-Al CLDH/BC	Bagasse	475 ℃	Tetracycline	1118.12	II	No	(X.F. Tan et al., 2016; X. Tan et al., 2016)
Mg-Al CLDH/BC	Ramie stem	500 ℃	CV[b]	374.686	II	24 h, 100 ℃	(X. Tan et al., 2016; X.F. Tan et al., 2016)
Mg-Al LDH/BC	Bovine bone	No	MB[b]	406.47	I	2 h	(Meili et al., 2019)
Ca-Al LDH/BC	Rice husk	No	MB[b]	32.535	I	3 d, 70 °C	(Lesbani et al., 2020)
Mg-Al LDH/BC	Date palm	700 ℃	MB[b]	302.75	I	24 h, 90 ℃	(Zubair et al., 2020)
Mg-Al LDH/BC	Syagrus coronate	400 ℃	DS[b]	82%	II	2 h	(de Souza dos Santos et al., 2020)
Ni-Al LDO/MBC	Corncob powder	700 ℃	AO[b]	116.3	III	24 h, 100 ℃	(Wang et al., 2020b)
Cu-Fe LDH/BC	Date palm	700 ℃	EBT[b]	565.32	I	24 h, 65 ℃	(Zubair et al., 2021b)
40% Mg–Al LDH/BC	Bamboo	600 ℃	Phosphate	> 95%	I	3 d, 80 ℃	(Wan et al., 2017)
Mg-Al LDH/BC	Sugarcane leaves	550 ℃	Phosphate	81.83	I	3 d, 80 ℃	(J. Li et al., 2016; R. Li et al., 2016)
Mg-Fe LDH/BC	Pinecone flakes	300 ℃	Phosphate	17.46	I	24 h, 70 °C	(Bolbol et al., 2019)
Mg-Al LDH/Hydrochar	Cottonwood	180 ℃	Phosphate	386	Others	12 h, 180 ℃	(Zhang et al., 2014)
Mg-Al-CLDH/BC	Rice husk	500 ℃	Phosphate	97.6%	II	3 d, 50 ℃	(Lee et al., 2019)
Mg-Al LDH/BC	Cotton Wood	600 ℃	Phosphate	410	I	3 d, 80 ℃	(Zhang et al., 2013)
Mg-Al LDOs/BC	Cabbage	500 ℃	Phosphate	127.2	II	6 h, 60 °C	(W. Zhang et al., 2019; Z. Zhang et al., 2019)
Mg-Al LDOs/BC	rape	500 ℃	Phosphate	132.8	II	6 h, 60 °C	(W. Zhang et al., 2019; Z. Zhang et al., 2019)
Mg-Al LDH/BC	Date-palm	700 ℃	Phosphate	177.97	I	24 h, 90 ℃	(Alagha et al., 2020)
Mg-Al LDH/MBC	CK[b]	600 ℃	Phosphate	252.88	Others	24 h, 80 °C	(Cui et al., 2019)
Zn-Al LDO/BC	Banana straw	500 ℃	Phosphate	185.19	III	8 h, 60 °C	(Jiang et al., 2019)
Zn-Al LDH/BC	Corn stalks	600 ℃	Phosphate	64.9	I, II	18 h	(Yang et al., 2019)
Ni-Fe LDH/BC	Corn stalks	600 ℃	Phosphate	78.3	I, II	18 h	(Yang et al., 2019)
Mg-Al LDH/BC	Corn stalks	600 ℃	Phosphate	152.1	I, II	18 h	(Yang et al., 2019)
Mg-Fe LDH/BC	Straw	600 ℃	Phosphate	206.2	II	4 h, 60 °C	(Rahman et al., 2021)
Mg-Fe LDH/BC	Wheat-straw	600 ℃	Nitrate	24.8	I	3 d, 70 ℃	(Xue et al., 2016)
Mg-Fe LDH@BC	Rice straw	600 ℃	Nitrate	27.09	I	24 h, 70 ℃	(H. Zhang et al., 2018; L. Zhang et al., 2018)
Mg-Al LDH/BC	Date-palm	700 ℃	Nitrate	28.06	I	24 h, 90 °C	(Alagha et al., 2020)
Mg-Al LDH/BC	Apple branch	500 ℃	Nitrate	156.84	I	4 h, 120 °C	(Wang et al., 2021)
Mg-Fe LDH@BC	Rice straw	600 ℃	NH_4^+	98.53	I	24 h, 70 °C	(H. Zhang et al., 2018; L. Zhang et al., 2018)
Ni-Fe LDH/BC	Pine	600 ℃	As(V)	4.38	I	80 °C, overnight	(Wang et al., 2016a)
Ni-Fe LDH/BC	Pine	600 ℃	As(V)	1.56	II	80 °C, overnight	(Wang et al., 2016a)
Ni-Mn LDH/BC	Pine	600 ℃	As(V)	6.52	I	80 °C, overnight	(Wang et al., 2016b)

(a) I, II and III represent post-pyrolysis method, pre-pyrolysis method and hydrothermal method respectively.
(b) SZ: Sulfamethoxa-zole, PSR: Pennisetum sinese roxb, CK: Caragana korshinskii, OCS: Oil-tea camellia shell, MB: Methylene blue, SC: Solidago canadensis EDTA: Ethylenediaminetetraacetic acid, AO: Acridine orange, CV: Crystal violet, DS: Diclofenac sodium, PBC: phosphate-impregnation biochar, EBT: Eriochrome black T.

Zhang et al., 2018; L. Zhang et al., 2018; Z. Huang et al., 2019; D. Huang et al., 2019; Y. Wang et al., 2018; C. Wang et al., 2018; T. Wang et al., 2018; Tan et al., 2019; Jia et al., 2019), organic contaminant (X. Tan et al., 2016; Meili et al., 2019; X.F. Tan et al., 2016; de Souza dos Santos et al., 2020), inorganic anions which included phosphate (Zhang et al., 2014; Yang et al., 2019) and nitrate (H. Zhang et al., 2018; L. Zhang et al., 2018; Alagha et al., 2020; Xue et al., 2016), arsenic (Wang et al., 2016a). As shown in Table 1, the maximum adsorption capacity for organic pollutant (tetracycline) was 1118.12 mg/g by Mg-Al LDO-BC composite, the maximum adsorption capacity for Pb(II) was 1264.10 mg/g by Mg-Fe LDH-BC composite, and the maximum adsorption capacity for phosphate was 410 mg/g by Mg-Al LDH-BC ultra-fine composites. All these reflected that LDH-BC composites were a kind of effective adsorbent for the removal of pollutants. Currently, the combination of LDHs and BC has been applied in Mg-Al LDH, Mg-Fe LDH, Ni-Fe LDH, Ni-Al LDO, Zn-Al LDO, Mn-Al LDH. Among them, Mg-Fe LDH-BC composite and Mg-Al LDH-BC composite were more widely applied (Table 1). In general, when LDH-BC composites were used as adsorbent, BC was regarded as a matrix mainly preventing the agglomeration of LDHs, and LDHs were mainly responsible for the adsorption of pollutants. Therefore, based on characteristics of target pollutants, we divided the mechanism of adsorption into three categories.

3.1.1. *Adsorption mechanisms of heavy metals*

3.1.1.1. Adsorption mechanisms of heavy metal cations. In general, the adsorption mechanisms of LDH-BC composites to heavy metal cations included isomorphic substitution, electrostatic interaction, complexation, and surface precipitation (Fig. 2). For instance, Mg-Fe LDH-Kiwi branch BC composite was used to adsorb Cd(II) through the complexation of amino, hydroxyl and carboxyl group of composite with Cd(II), the isomorphic substitution, and the surface precipitation (Tan et al., 2019). And the isomorphic substitution and the surface precipitation were regarded as main possible contribution to the removal of Cd(II). Besides, Jia et al. Jia et al. (2019) synthetized Mg-Fe LDH-magnetic biochar (MBC) composite as sorbent for Pb(II) removal. They concluded that surface co-precipitation between Pb(II) and interlayer CO_3^{2-}, and surface hydroxyl groups of hydrotalcite might be mainly conducive to the adsorption of Pb(II) by the precipitation of $Pb_3(CO_3)_2(OH)_2$ and $Pb(OH)_2$ (Fig. 2b). However, H. Zhang et al. (2018) and L. Zhang et al. (2018) summarized that the removal of Cd(II) and Pb(II) by Mg-Fe LDH@BC might be attributed to surface complexation and surface precipitation which seemed to dominate more than the former. Moreover, they concluded that the isomorphic substitution might contribute little to the removal of Pb(II) and Cd(II) because of their different ionic radius of Pb(II) (0.119 nm), Cd(II) (0.095 nm), Mg(II) (0.072 nm) respectively. Although they used Mg-Fe LDH/BC to adsorb Pb(II) and Cd(II), the concert mechanisms were controversial. On the one hand, because of the different biomass, synthesis method and experiment conditions, all these mechanisms might be valid. On the other hand, to the best of our knowledge, there were no LDHs prepared with lead or cadmium because of possible secondary pollution, and we didn't judge the rationalities and stabilities of Cd-Fe LDH and Pb-Fe LDH, and we also didn't know the specific effect of ionic radius on this isomorphic substitution. Therefore, the specific adsorption mechanisms of the removal of Pb(II) and Cd(II) were worth exploring. Except for the combinations of BC and Mg-Fe LDH, Mg-Al LDH-BC composite was also used as sorbent to capture Pb (II). Wang et al. (2020a) found that the main mechanism was complexations with functional groups and attracted through electrostatic force in the case of Pb(II) adsorption from a single system (Fu et al., 2021). Besides, Luo et al. (2020) concluded that the adsorption mechanism of Pb(II) by Mg-Al LDH-hydrochar composite might be mainly attributed to electrostatic effect and surface coprecipitation, and

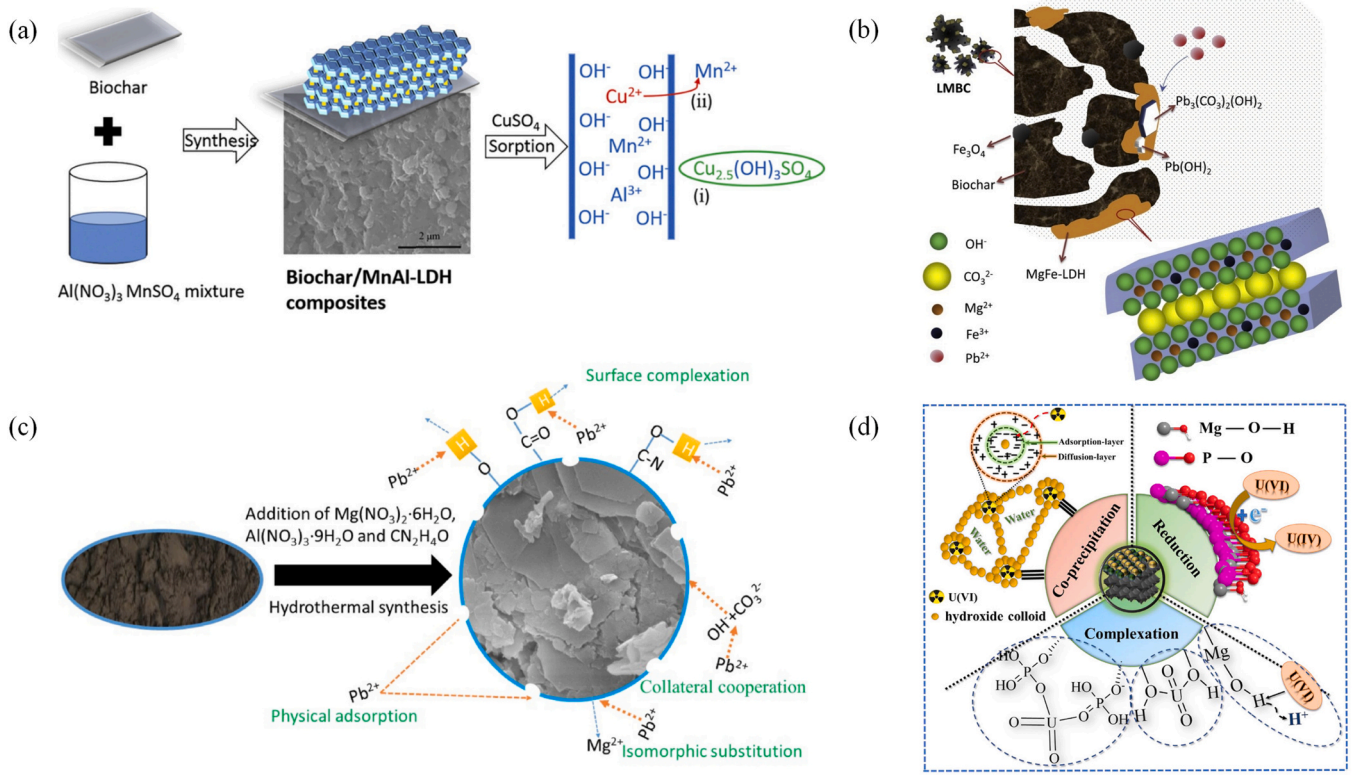

Fig. 2. The mechanisms for the adsorption of heavy metals. (a) Schematic diagram of adsorption mechanism of Cu(II) by Mn-Al LDH-BC (Y. Wang et al., 2018; C. Wang et al., 2018; T. Wang et al., 2018); (b) Schematic diagram of probable adsorption mechanism for Pb(II) removal by Mg-Fe LDH-MBC composite (Jia et al., 2019); (c) Schematic illustration of adsorption mechanism for Pb(II) by Mg-Al LDH-hydrochar composite (Luo et al., 2020); (d) Mechanism for the adsorption of U (VI) by Mg-Al LDH-PBC composite (Lyu et al., 2021).

physical adsorption was also a way to adsorb Pb(II) (Fig. 2c). Comparing two carbon-based composites synthetized by Mg-Fe LDHs and Mg-Al LDHs respectively, it could be found that the types of LDHs made a difference to the adsorption mechanisms because LDHs dominated the properties of LDH-BC composites (W. Zhang et al., 2019; Z. Zhang et al., 2019). In addition to Pb(II) and Cd(II), the removal of Cu(II) could be realized by Mn-Al LDH-BC composite. And the adsorption process involved surface precipitation of $Cu_{2.5}(OH)_3SO_4$ and the isomorphic substitution of Mn(II) with Cu(II) (Fig. 2a) (Y. Wang et al., 2018; C. Wang et al., 2018; T. Wang et al., 2018). Besides, the removal of Cu(II) could also be accomplished by surface complexation (H. Zhang et al., 2018; L. Zhang et al., 2018). Finally, it could be found that the removal mechanism of some metal ions has not been explored, such as Hg^{2+} and Ag^{+}, which is a research direction.

3.1.1.2. Adsorption mechanisms of metal oxide anions. At present, metal oxide anions removed by LDH-BC composites were associated with Cr (VI). The possible adsorption mechanisms of Cr(VI) were distinct from other heavy metals due to the forms of Cr(VI) in water and different reaction systems. In conclusion, the adsorption mechanisms of LDH-BC composites to Cr(VI) included interlayer anion exchange, electrostatic attraction, reduction, and isomorphic replacement. Z. Huang et al. (2019) and D. Huang et al. (2019) applied calcined ethylenediaminetetraacetic acid (EDTA)-Mg/Al LDH-BC composite to adsorb $Cr_2O_7^{2-}$, which was the main form of Cr(VI) in water. They found that electrostatic attraction and interlayer anion exchange dominated Cr(VI) sorption process. The former was mainly attributed to anionic clay, and the latter was caused by the memory effect. In other words, the surface layered double oxides of this calcined composite could recover original layered structure with anion embedded in the layered structure (X.F. Tan et al., 2016; X. Tan et al., 2016; El Gaini et al., 2009; Zhu et al., 2005). Moreover, M. Li et al. (2019) and G.W. Li et al. (2019) used Mg Al-LDH-BC composites to remove sulfamethoxazole and $Cr_2O_7^{2-}$ simultaneously, and they also concluded that interlayer anion exchange dominated the adsorption of Cr(VI). In addition to these mechanisms, some different mechanisms about the removal of Cr(VI) were discovered. Wang et al. (2020a) applied the engineered Mg-Al LDH-BC composite to simultaneously capture Pb^{2+} and CrO_4^{2-} from electroplating wastewater. They found that Cr(VI) of CrO_4^{2-} could be reduced to Cr^{3+} by functional groups of this composite which included C-C, C-O and C-N. And then the generated Cr^{3+} could replace the Al^{3+} in Mg-Al LDH via the isomorphic substitution due to their similar ionic radius (0.052 and 0.054 nm for Cr^{3+} and Al^{3+} ions, respectively) and closed surface charge density, consequently forming an Mg-Cr LDH structure (Wang et al., 2020a; Li et al., 2016). In the final analysis, we could draw the following conclusions about the removal of Cr(VI). Firstly, Cr(VI) could be removed in the forms of anions (CrO_4^{2-}, $Cr_2O_7^{2-}$) and trivalent cation (Cr^{3+}) which caused the isomorphic substitution from Al^{3+} to Cr^{3+} to reconstruct Mg-Al LDH in LDH-BC composite. Secondly, the synergetic effect was propitious to the adsorption of Cr(VI). In details, Pb^{2+} could form complexations with carbonate species and this would let more CO_3^{2-} release into solution from interlayer of LDH and led to forming more vacancies which was highly attractive to CrO_4^{2-} species (Wang et al., 2020a).

3.1.1.3. Adsorption mechanisms of radionuclides. Some radionuclides in wastewater posed threat to ecological environment and human health, such as U(VI), Eu(III), Cs(I), Cm(III), Sr(II), Am(III), Np(IV) and Pu(IV) (Liu et al., 2021a, 2021b; Pang et al., 2018; Dai et al., 2019; Zhong et al., 2020; Qiu et al., 2021; Wang et al., 2020). At present, LDH-BC composites have been used to remove radionuclides (e.g., Eu(III), U(VI)) in wastewater treatment. In the whole, the adsorption mechanisms of LDH-BC composites to radionuclides included ion exchange, complexation, precipitation, and reduction reaction. For example, Mg-Al LDH/phosphate-impregnation-BC (Mg-Al LDH/PBC) composite was used to adsorb U(VI) and the maximum adsorption capacity of U(VI) by Mg-Al LDH/PBC composite was an improvement of ~17 times than that of unmodified biochar (Lyu et al., 2021). As shown in Fig. 2d, the high adsorption efficiency by Mg-Al LDH/PBC composite was attributed to the following mechanisms: (1) the co-precipitation of polyhydroxy aluminum cations removing U(VI), (2) the surface complexation with U (VI) because of surface functional groups (P–O, Mg/Al–O–H, and –OH), (3) the reduction of U(VI) to U(IV) due to the adequate electronic donors (e.g., P–O, Mg–O–H). X. Li et al. (2020) and S.B. Li et al. (2020) achieved the removal of Eu(III) from wastewater by Ca-Al LDH-BC composite and the theoretical maximum adsorption amount of Eu(III) was up to 120.482 mg/g (Table 1). And three mechanisms were involved in the Eu (III) sorption, including complexation with oxygen-containing functional groups (e.g., C-O, C═O, -OH), ion exchange between Al(III) and Eu(III) ions, and co-precipitation. In conclusion, LDH-BC composites have high adsorption efficiency in the removal of radionuclides and more studies should be paid to this aspect.

3.1.2. Adsorption mechanisms of organics

Organic pollutants were complex substances that usually contained functional groups such as benzene ring, hydroxyl group and amino group, which were closely related to the mechanism of pollutant removal (X.F. Tan et al., 2016; X. Tan et al., 2016). In conclusion, the main adsorption mechanism of these organic pollutants could be summarized as four types: electrostatic attraction, anion exchange, hydrogen bond and π-π interaction (Fig. 3a, b) (X. Tan et al., 2016; X.F. Tan et al., 2016). For the first adsorption mechanism, taking acridine orange (AO) and crystal violet (CV) as examples, Wang et al. (2020b) used Ni-Al layered double oxides (LDOs)-MBC composite to remove AO. It could be found that the electrostatic interaction was the main adsorption driving force of Ni-Al LDOs-MBC composite for AO. AO was an alkaline dye, which could dissociate cations by protonation, and the surface of Ni-Al LDOs-MBC composite was negatively charged in an alkaline environment (Wang et al., 2020b). Therefore, this composite could adsorb AO by electrostatic interaction. X. Tan et al. (2016) and X. F. Tan et al. (2016) applied Mg-Al calcined layered double hydroxide (CLDH)-BC composite as sorbent for the removal of CV. The deprotonation of various surface functional groups and an increase in the pH of the solution due to anion exchange might be propitious to make the surface of Mg-Al CLDH-BC composite negatively charged, which contributed to the electrostatic interaction between this composite and CV cations (X. Tan et al., 2016; X.F. Tan et al., 2016). In addition, part of CV could dissociate to CV anions in a specific pH range (near 8.8) and embedded into the interlayer space in the reconstructed Mg-Al LDH, which was the second mechanism (anion exchange) (X. Tan et al., 2016; X.F. Tan et al., 2016; Chen et al., 2009). X.F. Tan et al. (2016) and X. Tan et al. (2016) used Mg-Al LDO-BC composite to adsorb Tetracycline (TC), mainly with the form of anionic species (TCH^- or TC^{2-}) in a certain alkaline environment. And TCH^- or TC^{2-} could be intercalated into the interlayer space to reconstruct Mg-Al LDH-BC composite from Mg-Al LDO-BC composite (Fig. 3a). From the above, we knew that the adsorption mechanisms were related to the form of contaminant in the reaction solution, and the pH value of the reaction solution had a great influence on the mechanism analysis. The third mechanism was hydrogen bond, which was a special intermolecular or intramolecular interaction between hydrogen atom and other atoms such as oxygen, fluorine, and nitrogen. Specifically, organic contaminants consist of hydroxyl and amino and other groups, and the surface of this composite had many functional groups, (e.g., hydroxyl and alkoxy groups). These functional groups between this composite and contaminant contributed to the formation of hydrogen bond (Fig. 3a, b). The fourth mechanism was π-π interaction which was formed by conjugation between the C═C of the composite materials and the benzene ring of pollutant (X.F. Tan et al., 2016; X. Tan et al., 2016; Yu et al., 2017). In addition to these main mechanisms, as shown in Fig. 3b, organic contaminants might be adsorbed in the pore of composite through physical

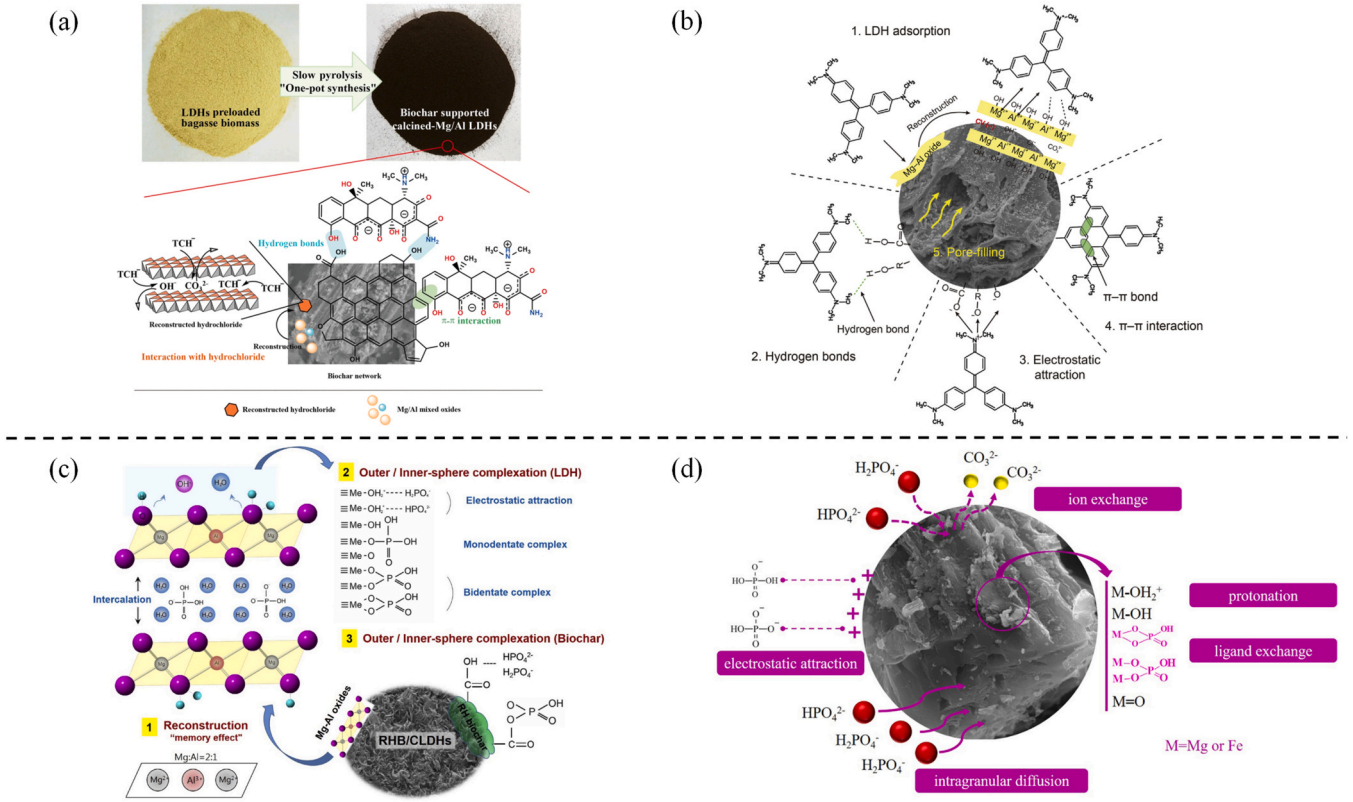

Fig. 3. The mechanisms for the adsorption of organic contaminants and phosphate. (a) Schematic illustration of adsorption mechanisms for tetracycline by calcined-Mg-Al LDH-BC composite (X.F. Tan et al., 2016; X. Tan et al., 2016); (b) Adsorption mechanisms of CV by calcined Mg-Al-LDH-BC composite (X. Tan et al., 2016; X.F. Tan et al., 2016); (c) Schematic illustration of possible mechanisms for phosphate adsorption by the example of Mg-Al CLDH-RHB composites (Lee et al., 2019); (d) Illustration of phosphate recovery mechanism by Mg-Fe LDH-BC (Liu et al., 2021).

adsorption-pore-filling (Wang et al., 2020b).

3.1.3. Adsorption mechanisms of inorganic anions

3.1.3.1. Adsorption mechanisms of phosphate. Inorganic anions mainly include phosphate, nitrate, ammonium, and arsenic. Among them, nitrogen, phosphorus, and arsenic belong to same main group in the periodic table, and there are many similarities in their properties. Therefore, their adsorption mechanisms can be summarized and discussed together.

In conclusion, the main mechanism of phosphate removal could be summarized as three points: the anion exchange or ion exchange, the electrostatic attraction and complexation. Memory effect played an important role in the phosphorus adsorption mechanism of LDOs-BC composites (Lee et al., 2019; Zhang et al., 2019). The LDHs were transformed into LDOs during calcination process while BC was being prepared. Phosphate could be intercalated into the interlayer space to reconstruct LDHs from LDOs and acted as a balance of charge because of its electronegativity. Besides, it's worth emphasizing that the result of this mechanism was like that of anion exchange (Fig. 3c). For the uncalcined LDH-BC composites, the interlaminar anions could generally be chlorine ion, nitric acid and carbonate, and phosphate anions could exchange with these interlaminar anions to enter the interlaminar structure of LDHs during adsorption (Fig. 3d) (J. Li et al., 2016; R. Li et al., 2016; Wan et al., 2017; Jiang et al., 2019; Bolbol et al., 2019; Cui et al., 2019). Electrostatic attraction was another mechanism which contributed to the fast adsorption of phosphate and it was affected by the type of material and the reaction environment (Cui et al., 2019). In details, when the pH value of reaction solution was lower than the isoelectric point (pH_{ZPC}), the surface hydroxyl of this composite was protonated and was positively charged (Jiang et al., 2019; Bolbol et al., 2019; Liu et al., 2008). So, phosphate, mainly in the form of anions (e.g., $H_2PO_4^-$, HPO_4^{2-}), could interact with the surface hydroxyl of this composite by electrostatic attraction (Fig. 3c, d). Another mechanism was complexation, which was directly related to the two above-mentioned mechanisms. The anion exchange and the electrostatic attraction could attract phosphate anions to the surface or between the layers of the composite, and then the phosphate would interact with the functional groups via ligand exchange (J. Li et al., 2016; R. Li et al., 2016; Lee et al., 2019; Cui et al., 2019). Though inner-sphere monodentate surface complex and inner-sphere bidentate surface complex were shown in Fig. 3c, these were just some of the complexes overall. And the outer/inner-sphere surface complexes could be formed by the interaction of phosphate with functional groups in CLDHs and BC, respectively (Lee et al., 2019). The outer/inner-sphere surface complexes in CLDHs could be divided into monodentate complex and bidentate complex that was further divided into bidentate-mononuclear complex and bidentate-binuclear complex (Fig. 3c). In addition to these above mechanisms, intraparticle diffusion might also be a factor controlling the adsorption process. In detail, phosphate could gradually diffuse to the inner pore of BC when active sites on the surface LDH-BC composites were gradually occupied (Fig. 3d) (Liu et al., 2021).

3.1.3.2. Adsorption mechanisms of nitrate and ammonium ion. The existing forms of nitrogen in wastewater usually were nitrate (NO_3^-) and ammonium ion (NH_4^+). As shown in Fig. 4a, LDH of composites was the dominated adsorption site. For the removal of NH_4^+, the hydrogen bonding might be the main mechanism. Although NH_4^+ was positively charged, which might have a negative influence on the adsorption by LDH-BC composites because of the electrostatic repulsion, the hydrogen bond between NH_4^+ and O—H was stronger than the electrostatic repulsion (H. Zhang et al., 2018; L. Zhang et al., 2018). For the removal

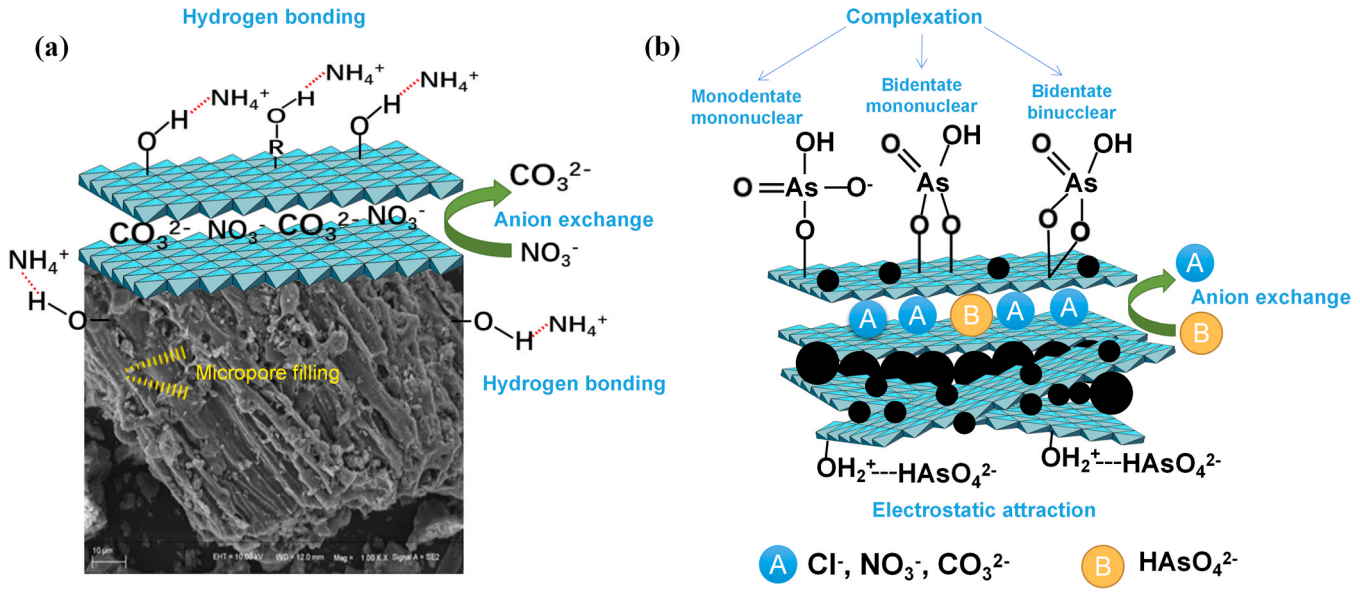

Fig. 4. (a) Schematic diagram of mechanisms of LDH-BC composites adsorbing NO_3^- and NH_4^+; (b) Schematic diagram of mechanisms of LDH-BC composites adsorbing $HAsO_4^{2-}$.

of NO_3^-, LDHs in composite materials were mainly Mg-Fe LDHs and Mg-Al LDHs, and the main mechanisms were the anion exchange (Fig. 4a) (H. Zhang et al., 2018; L. Zhang et al., 2018; Alagha et al., 2020). Because the anion exchange mainly took place in LDHs of LDH-BC composites, different LDHs had different adsorption effects on nitrate. It had been confirmed that Mg–Fe LDHs had relatively higher selectivity for nitrate (0.29 nm) adsorption than Mg-Al LDHs because of its suitable interlayer spacing for fixing NO_3^- (H. Zhang et al., 2018; L. Zhang et al., 2018; Xue et al., 2016; Tezuka et al., 2004). Therefore, Mg-Fe LDH-BC composites showed a high selectivity for nitrate. For the other mechanism, the micropore filling by van der Waals force might play an important role in NO_3^- adsorption because the molecular size of NO_3^- was close to the pore size of BC and Mg-Fe LDH composite (Fig. 4a) (H. Zhang et al., 2018; L. Zhang et al., 2018; Lian et al., 2016). In conclusion, these mechanisms could be summarized as three aspects: the anion exchange, complexation and electrostatic attraction (Wang et al., 2016a).

3.1.3.3. Adsorption mechanisms of arsenic. At present, As(V) ($HAsO_4^{2-}$) could be removed by LDH-BC composites, and the adsorption mechanisms included complexation, electrostatic attraction and anion exchange (Wang et al., 2016a, 2016b). As(V) could form specific complexes with hydroxyl functional groups (-OH) of the part of LDH, and mechanisms on forming complexes with $HAsO_4^{2-}$ included monodentate mononuclear, bidentate mononuclear and bidentate binuclear (Fig. 4b). Although complexation could occur between $HAsO_4^{2-}$ and -OH on BC surface, the adsorption capacity was low and might be negligible compared to the part of LDH (Wang et al., 2016a, 2015). When the experimental pH was higher than the point of zero charge, the LDH surface was positively charged due to protonation of -OH, which could adsorb $HAsO_4^{2-}$ by electrostatic attraction (Fig. 4b). What's more, anion exchange was also involved in adsorption of $HAsO_4^{2-}$ (Goh et al., 2009; Chetia et al., 2012). And $HAsO_4^{2-}$ could exchange with anions (e.g., Cl^-, NO_3^-, CO_3^{2-}) in the interlayer of LDH (Fig. 4b).

3.2. Application of LDH-BC composites in catalysis

3.2.1. Photocatalysis and sonocatalysis

Only a few studies were about the application of LDH-BC composites in photocatalysis and sonocatalysis. Gholami et al. (2020b) successfully synthesized Fe-Cu LDH-BC composite with enhanced sonocatalytic activity for 97.6% degradation rate of cefazolin sodium, and Zn-Co-LDH@BC nanocomposite exhibited 92.7% degradation rate for gemifloxacin through photocatalysis (Gholami et al., 2020a). What's more, Mn-Fe LDO-BC composite was used to remove tetracycline (TC) and the degradation rate of TC reached 98% within 240 min upon exposure to a UV light (Azalok et al., 2021a). The high degradation rate of cefazolin sodium in the sonocatalysis could be attributed to the sonoluminescence phenomena which referred to light emission through the recombination of free radicals that result from cavitation bubbles (Gholami et al., 2020b; Khataee et al., 2018a, 2018b). And this light was in the ultraviolet range and was capable of exciting the Fe-Cu LDH-BC composite as photocatalyst during the ultrasonication. Therefore, the degradation mechanisms of cefazolin sodium and gemifloxacin (GMF), and TC were similar. In details, the UV irradiation could create hole (h^+) and photogenerated electron (e^-) on surface of LDH-BC composites (Fig. 5c) (Gholami et al., 2020a, 2020b; Azalok et al., 2021a, 2021b). The h^+ could react with H_2O to produce •OH or could oxidize organic pollutants directly (Fig. 5d). Whereas, the photogenerated e^- could capture dissolved oxygen to yield $O_2^{\bullet-}$ which was subsequently protonated to produce H2O2 and further form •OH (Fig. 5c). Finally, pollutants could be oxidated by those generated radicals. What's more, in the presence of $K_2S_2O_8$, the degradation efficiency of contaminants could be improved because the photogenerated e^- can react with $S_2O_8^{2-}$ to produce the highly selective $\bullet SO_4^-$ radicals (Fig. 5c) (Gholami et al., 2020b; Azalok et al., 2021a, 2021b; Golshan et al., 2018; Wang et al., 2017; Shao et al., 2017).

In this process, active reaction sites are mainly distributed in LDHs, and BC particles can reduce the agglomeration of LDHs and expose more active reaction sites to react with active substances, thus improving the removal efficiency of pollutants. What's more, BC can also block the recombination of h^+ and e^-, enhancing the photocatalytic activity (Gholami et al., 2020a, 2020b).

3.2.2. Fenton reaction

At present, LDH-BC composites had a few applications in Fenton or Fenton-like reaction. For instance, Fe-Al LDH-BC was used to remove phenol by the activation of H_2O_2 and the degradation efficiency could be up to 85.28% (Fan et al., 2021). In the degradation process, H_2O_2 could accept the electron from the redox of Fe (II) to produce Fe (III) on the surface of LDHs to produce •OH which would oxidate pollutants directly and realized the degradation effectively (Fig. 5b). Besides, •OH could

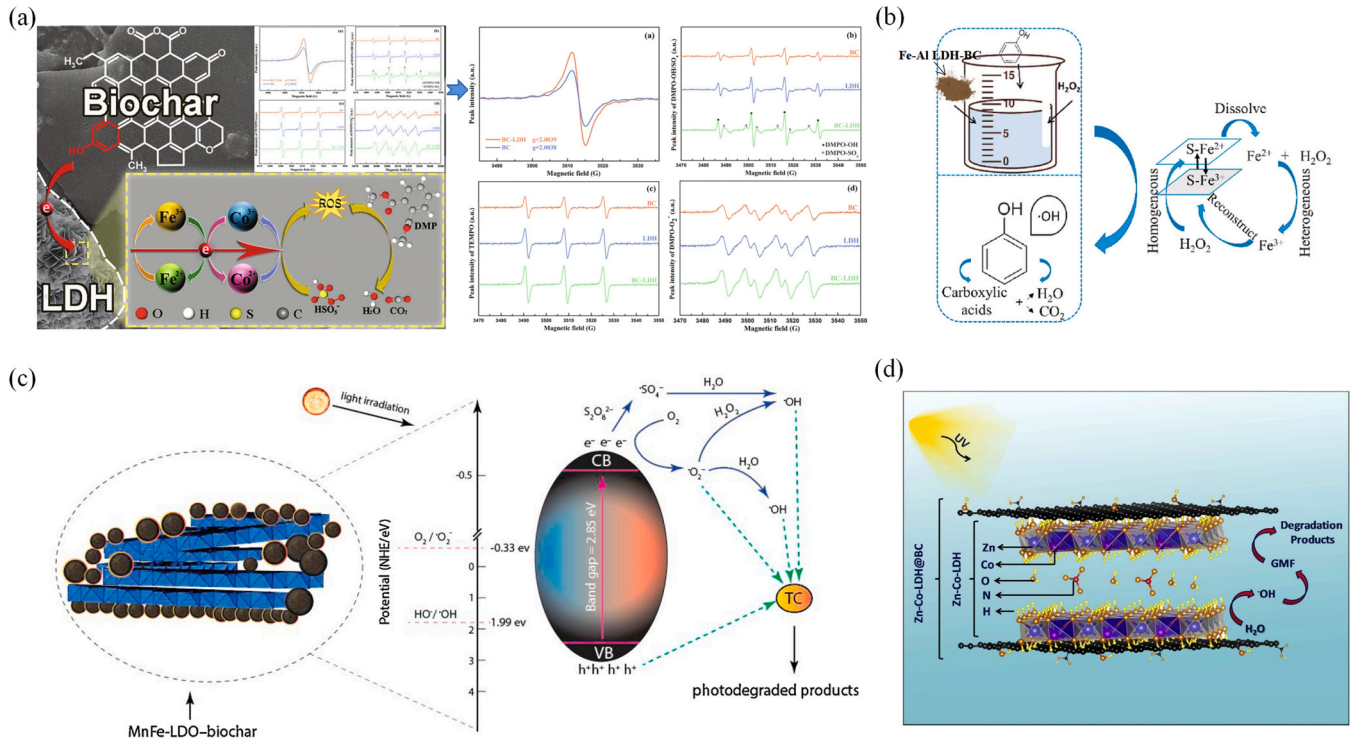

Fig. 5. The schematic diagram of mechanisms of LDH-BC composites in catalysis. (a) the reaction mechanism of Co-Fe LDH-BC composite/PMS system and the identification of different ROS (Ye et al., 2021); (b) the schematic diagram of Fe-Al LDH-BC composite/H_2O_2 system (Fan et al., 2021); (c) probable mechanism for TC degradation via photocatalytic reaction using Mn-Fe LDO–BC composite (Azalok et al., 2021a); (d) the schematic diagram for degradation of GMF using Zn-Co LDH-BC composite (Gholami et al., 2020a).

further react with H_2O_2 to generate $O_2^{\bullet-}$ (Fan et al., 2021; Q. Yang et al., 2021). In addition to H_2O_2, peroxymonosulfate (PMS) could also be activated by LDH-BC composites to produce reactive oxygen species. For example, 100% of dimethyl phthalate (DMP) degradation efficiency was achieved in Co-Fe LDH-BC composite/PMS system within 60 min, while only 62% in Co-Fe LDH/PMS system (Ye et al., 2021). In the degradation process of DMP, PMS was activated to produce reactive oxygen species (ROS) (persistent free radicals, •OH, $SO_4\bullet^-$, $^1O_2$, $O_2\bullet^-$) when its peroxide bond (-O-O-) was cleaved by accepting one electron from Fe(II) or Co(II) (Fig. 5a) (H. Qin et al., 2020; J. Qin et al., 2020; F. Qin et al., 2020). Although the catalytic process was mainly on the surface of the LDHs part, BC also played an important role in all process. Firstly, BC could act as an electron carrier (D. Huang et al., 2019; Z. Huang et al., 2019; Kappler et al., 2014; Ye et al., 2020). Secondly, LDHs were attached to the surface of BC and BC could reduce the leaching of metal ions, which was propitious to the repeatability of LDH-BC composites.

LDH-BC composites or LDO-BC composites were regarded as the potential catalysts in wastewater treatment by advanced oxidation processes (photocatalysis, Fenton reaction methods, and sulfate radical-mediated oxidations) due to their porous structure, large surface area, wide tunability of the types of metal cations, and the nature of interlayer compensating anions. However, LDH-BC composites or LDO-BC composites are not widely used in catalysis. More attempts are needed in designing and fabricating high catalytic activities LDH-BC based catalysts with superior physicochemical properties and synergistic effects. And LDH-BC composites should be used to degrade a wider range of organic contaminants and the degradation mechanisms of pollutants need to be further studied.

3.3. Other applications of LDH-BC composites in wastewater treatment

Based on the excellent adsorption efficiency, LDH-BC composites could be used as a kind of filler in fixed-bed column for simulated wastewater treatment (Wang et al., 2020a; Rahman et al., 2021). For instance, wang et al. Wang et al. (2020a) concluded that 1 kg of Mg-Al LDH-BC composite could treat 3.8 and 3.1 tons of Pb^{2+} and CrO_4^{2-} wastewater after the fixed-bed column studies. This indicated that LDH-BC composites were a kind of cost-effective and efficient material on wastewater purification and had a good prospect in commercial application. What's more, LDH-BC composites could also be prepared as an immobilized carrier for microorganism. For example, Mg-Al LDH-BC composite combined with sodium alginate was successfully used as an immobilized carrier for *Acinetobacter* sp. FYF8 to increase the removal efficiency of phosphorus and nitrogen in the bioreactor (Zheng et al., 2021). This material was convenient for recycling and would not cause secondary pollution (Xiao et al., 2019; Zheng et al., 2021). It indicated that LDH-BC composites had potential as immobilized carrier in biological method for wastewater treatment. And more studies should be focused on this aspect.

Compared with traditional materials (e.g., activated carbon, silica gel and organic materials (Su et al., 2019)), LDH-BC composites have many advantages in commercial applications when they are used as filler or as carrier for microbial immobilization. Firstly, LDH-BC composites have a high removal efficiency for various pollutants (e.g., heavy metals, organic contaminants, nitrate and phosphate), which indicates that LDH-BC composites have a wide range of applicability in commercial applications. Secondly, the LDH-BC composites have an advantage in reusability, which is helpful to reduce the frequency of changing packing in fixed-bed column and reduce the operating cost (X. Tan et al., 2016; Meili et al., 2019; X.F. Tan et al., 2016). Thirdly, BC is a kind of sustainable material with a wide range of sources and low price (Tan et al., 2015). So LDH-BC composites can provide a circular economy way to realize the recycling of agricultural waste and greatly reduce the production cost in commercial applications (Rahman et al., 2021). In addition, some LDH-BC composites adsorbing phosphate can be used as good slow-release fertilizer in some alkaline soils (Rahman et al., 2021).

To sum up, the high-performance sorbent LDH-BC composites have potential market value, which can be packaged into like-activated carbon products in supermarkets and realize its economic value (Wang et al., 2021). We think that LDH-BC composites have great potential in commercial application, and more research should be developed in this aspect.

4. Strategies for enhancing the properties of LDH-BC composites

According to the existing literatures, some modification strategies for enhancing the properties of LDH-BC composites had been used in the synthesis of LDH-BC composites. We will discuss these from two perspectives of biochar and LDH, including magnetic treatment, acid treatment, alkali treatment, modification of LDHs, controlling metal ion ratios, and calcination (Fig. 6). In addition to these strategies, other modification methods are also used in the synthesis of LDH-BC composites (e.g., ternary LDHs; Shafiq et al., 2020), phosphate-impregnation biochar (Lyu et al., 2021)). However, there is less research about these modification measures and further investigations are needed. Therefore, we will be focus on the following six modification measures based on the publication time and quantities of relevant literatures.

4.1. Modification of BC

4.1.1. Magnetic treatment

For the LDH-MBC composites, magnetization processes applied in the synthesis were related to $FeCl_2$ solution, $FeCl_3$ solution or iron electrodes (Wang et al., 2020b; Jia et al., 2019; Cui et al., 2019). Although these magnetization processes were different, they all used a reagent or material related to iron, which was also the core of the preparation of LDH-MBC composite. In addition to iron, the magnetic species applied to the magnetic BC mainly included nickel chloride ($NiCl_2$), manganese chloride ($MnCl_2$), cobalt chloride ($CoCl_2$) (Yi et al., 2020). With the advantages of low cost and environmental harmlessness, iron salts were widely used (Yi et al., 2019; L. Zhang et al., 2018; H. Zhang et al., 2018; Li et al., 2019). Compared with LDH-BC composites, some advantages made LDH-MBC composites more competitive. Firstly, LDH-MBC composites could be centrally recovered by magnetic field. The recovery process was simple, no secondary pollution (Yi et al., 2020; G.W. Li et al., 2019; M. Li et al., 2019; Yap et al., 2017; Son et al., 2018). Secondly, higher surface area and pore volume of LDH-MBC composites were contributed to remove contaminant by the mechanism of pore-filling (Yi et al., 2020; G.W. Li et al., 2019; M. Li et al., 2019; Zhao and Lang, 2018). Thirdly, •OH and $SO_4^{\bullet-}$ radicals might be generated by active sites such as Mn^{2+} and Fe^{2+} on the catalyst surface in the Fenton and Fenton-like systems. And Fe^{2+} in other materials doped with Fe_3O_4 was proved as an active site for catalysis (F. Qin et al., 2020; J. Qin et al., 2020; H. Qin et al., 2020; C. Chen et al., 2019; C.R. Chen et al., 2019; G. Chen et al., 2019; Zhu et al., 2019; Duan et al., 2020; Wang et al., 2020). What's more, the mechanisms of activation of H_2O_2 and peroxymonosulfate (PMS) by Mn^{2+} and Fe^{2+} to generate free radicals were similar. In the process of metal transformation from divalent state to trivalent state, electrons were transferred to PMS or H_2O_2, thus generating free radicals to degrade pollutants (C. Chen et al., 2019; C.R. Chen et al., 2019; G. Chen et al., 2019). Therefore, it could be speculated the catalytic effect of LDH-BC composites could be improved after using manganese salt or iron salt to synthesize LDH-MBC composites. Although magnetization processes for the synthesis of magnetic BC used in the synthesis of LDH-MBC composites were related to iron salts, the essence of these magnetization processes were the conversion from iron ions to Fe_3O_4 and the combination of Fe_3O_4 and BC (Wang et al., 2020b; Jia et al., 2019; Cui et al., 2019; G.W. Li et al., 2019; M. Li et al., 2019; Son et al., 2018; Shan et al., 2014). In the synthetic methods, calcination, co-precipitation and pyrolysis were often used to synthetize magnetic BC (S.B. Li et al., 2020; X. Li et al., 2020; Thines et al., 2017).

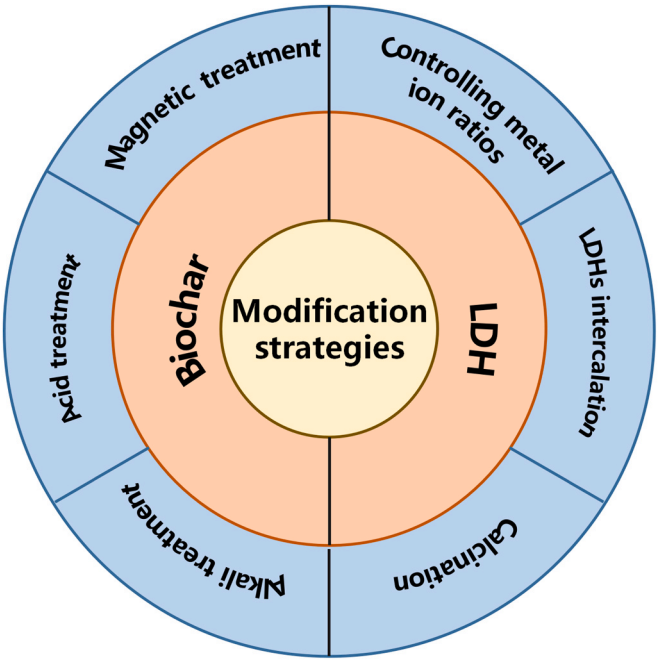

Fig. 6. The summary diagram of modification strategies.

4.1.2. Acid treatment

During the synthesis process of LDH-BC composites, BC could be oxidized by acid treatment, such as a mixture containing sulfuric acid and nitric acid (3:1 v:v), which was an effective modified strategy for improvement of properties of LDH-BC composites (Gholami et al., 2020b). With acid treatment, carboxyl and hydroxyl groups were introduced onto BC surface. Besides, acid treatment could affect the surface negative charge of the BC because of increased functional groups (Tan et al., 2020). Although most BC were alkaline and the surfaces of BC were mainly negatively charged (F. Qin et al., 2020; H. Qin et al., 2020; J. Qin et al., 2020), the surface of the BC treated with acid treatment was more electronegative. Therefore, the electrostatic interaction between BC and LDHs was more stable, which indirectly increased the stability of the LDH-BC composites. In details, the surface of LDHs was positively charged and had a strong attraction to electronegative materials. BC treated with acid was negatively charged and could combine with LDHs by electrostatic interaction, which might also increase the dispersion of LDHs on BC matrix. Finally, impurities (e.g., metallic residues) on the surface of BC could be removed by acid treatment (Zoroufchi Benis et al., 2020). At present, LDH-BC composites synthesized from the negatively charged BC only had application in catalysis, and had no relevant application in the field of adsorption. The feasibility of application in adsorption was worth exploring because the negative BC might be propitious to improve the adsorption efficiency of LDH-BC composites for some cations by electrostatic attraction (W. Zhang et al., 2020; C. Zhang et al., 2020; M. Zhang et al., 2020), such as ammonium and heavy metal cations. Of course, the actual effect of LDH-BC composites with acid treatment depended on the practical studies, so this remained to be studied experimentally.

4.1.3. Alkali treatment

Based on published papers, some alkaline chemical reagents could be used to modify the BC, such as KOH, NaOH, Na_2CO_3 and K_2CO_3 (H. Zhang et al., 2018; L. Zhang et al., 2018Xiao et al., 2018; Cha et al., 2016; Wang et al., 2019). It could be found that these alkaline chemical reagents had similar effects on BC. Firstly, the alkali pretreatment could increase the porosity and specific surface area of BC (Zoroufchi Benis et al., 2020; Xiao et al., 2018). Taking sludge BC with thermal-alkaline pretreatment for example, the surface area, total pore volume,

micro-pore volume and average pore diameter of the solids of thermal-alkaline pretreated sewage sludge (RSTAS)-BC increased by 43.5%, 33.3%, 23.1%, and 6.2% respectively (Xiao et al., 2018). Regarding the mechanism of activation of BC by alkaline chemicals, taking KOH as example, K_2O or K_2CO_3 produced by KOH increased the surface area and porosity by separating the carbon layer on the surface of BC (Zoroufchi Benis et al., 2020; Cha et al., 2016), which could also significantly improve the BC's crystallinity (Z. Yang et al., 2016; X. Yang et al., 2016). On the one hand, this measure was conducive to increasing the contact area between BC and LDHs, so more LDH particles could combine with BC, and the yield of LDH-BC composites could be improved. On the other hand, the development of porosity might contribute to the adsorption effect in pore-filling. Secondly, the alkali-treated BC had a lower C content and a higher O/C ratio than raw BC, which indicated that the alkali-treated BC might be more hydrophilic and might increase adsorption amount for hydrophilic contaminants (Xiao et al., 2018; J. Wang et al., 2019; X.H. Wang et al., 2019; M. Wang et al., 2019; Chen et al., 2011; Dong et al., 2011; Han et al., 2016). Third, the alkali treatment would increase the functional groups on the surface of BC, such as -OH, -COOH, -C═O (Fan et al., 2010; Jin et al., 2014). And OH and -COOH on the surface of BC would increase the hydrophilicity of LDH-BC composites and -C═O was propitious to the PDS decomposition in catalysis.

4.2. Modification of LDHs

4.2.1. Controlling metal ion ratios

In LDH-BC composites, LDHs with different metal ion ratios might have an influence on the adsorption efficiency of pollutants. Meili et al. (2019) used Mg-Al LDH-BC composites with different molar ratios of Mg/Al (2:1, 3:1 and 4:1) to remove methylene blue (MB) by adsorption. The results showed that there was almost no difference among three proportion materials on the kinetic tests. Mg-Al CLDH-BC composites (the metal ion ratio were 2:1 and 5:1) were synthesized by Lee et al. (2019) to adsorb phosphate, and composite with metal ion ratio (2:1) showed higher phosphorus removal efficiency. However, J. Li et al. (2016) and R. Li et al. (2016) applied Mg-Al LDH-BC with different Mg/Al ratios (2:1, 3:1, 4:1) to adsorb phosphate and found that 4:1 Mg/Al LDH-BC had the maximum adsorption capacity. The properties of LDH-BC composites were affected by different ion ratios. Firstly, the surface area increased, and the volume and diameter of the pores decreased with the increasing of the Mg/Al molar ratio, which could be attributed to the nanoparticles of LDH being supported on the pores of the BC (Meili et al., 2019; Valletregi, 2004). Secondly, the charge density of Mg-Al LDH-BC became weaker as the Mg/Al ratio increases. On the one hand, the weaker charge density might make phosphate ions easier to access the increased interlayer space (J. Li et al., 2016; R. Li et al., 2016; Wan et al., 2012), which could be used to explain why the composite with 4:1 metal ion ratio showed best adsorption capacity. On the other hand, the decrease of the charge density might affect anion exchange and further decrease the phosphate adsorption efficiency, because the anion exchange in LDH of LDH-BC composites was mainly based on the magnitude of electrostatic attraction between the positively charged LDH layers and the exchangeable anions in the interlayer region and bulk solution (Lee et al., 2019; Oestreicher et al., 2014; Khan et al., 2018). Although both interlayer distance and charge density could affect phosphate adsorption, it was difficult for us to compare the two factors according to the existing literature due to the different experimental conditions. According to the research about LDH-BC composites with different metal ion ratio used in the adsorption of contaminants, it could be deduced that LDH-BC composites with different metal ion ratios had selective adsorption efficiency for pollutants. Therefore, the selection of LDH-BC composites with appropriate metal ion ratios would broaden application of LDH-BC composites in wastewater treatment.

4.2.2. LDHs intercalation

EDTA intercalated LDH was a method to modify LDH-BC composites (Z. Huang et al., 2019; D. Huang et al., 2019; Wang and Wang, 2018). However, due to the different synthesis methods, the specific effects of EDTA in changing properties and affecting adsorption effect of LDH-BC composites were different. For the LDH-BC composites which had not been calcined at high temperature, EDTA functionalized LDHs significantly improved the adsorption efficiency of heavy metal cations, which could be attributed to the chelation between heavy metal cations and EDTA anions in the interlayer of LDHs (Y. Wang and Y. Wang, 2018; T. Wang and T. Wang, 2018; C. Wang and C. Wang, 2018; Kameda et al., 2005; Rojas et al., 2009). For the CLDH-BC composites or LDO-BC composites, Z. Huang et al. (2019) and D. Huang et al. (2019) used BC modified with Mg-Al LDH intercalated with EDTA composite to remove Cr(VI). They found that the calcination products of EDTA were present in the composites after calcination, which increased the number of functional groups (e.g., N-H) of LDH-BC composites. It could be seen that modification of LDHs in the composite with EDTA could improve the overall properties of the composite material, no matter for the calcined composite material or the non-calcined material. Therefore, using EDTA to intercalate LDHs was an effective measure to improve the performance of LDH-BC composites. Other chelating agents could be intercalated in pure LDHs, such as mercaptocarboxylic acids (Nakayama et al., 2007), tartrate (Kameda et al., 2008), diethylenetriaminepentaacetate (DTPA) (Pavlovic et al., 2009). But whether these chelators can be used to synthesize LDH-BC composites remains to be explored.

4.2.3. Calcination

Combining the research on LDH-BC composites and LDHs application, it could be found that the properties of composites produced by the modified liquid-phase deposition method had been significantly improved. In details, LDHs on composite could be converted into corresponding mixed metal oxide (MMO) or LDO after calcination, which might be propitious to the adsorption effect of LDH-BC composites. Besides, Zhang et al. concluded that MMO with uniform distribution (M^{2+} and M^{3+}) showed the higher surface area after calcination which was a very promising candidate in the photocatalytic application (Yang et al., 2020; Zhang et al., 2019). It could be attributed to the efficient electron transfer of the unsaturated metals, the new formation of photocatalytic nanocrystals (X. Yang et al., 2016; Z. Yang et al., 2016; Yang et al., 2020; Y. Wu et al., 2018; M.J. Wu et al., 2018; G. Chen et al., 2019; C.R. Chen et al., 2019; C. Chen et al., 2019; Lan et al., 2013). Therefore, LDO-BC composites may also be a good catalyst in the photocatalytic application which is worth exploring.

We mainly discuss modification measures of LDH-BC composites from six aspects (Fig. 6). However, other measures have the potential to improve the properties of LDH-BC composites (e.g., ternary LDHs and phosphate-impregnation biochar), and more studies should be focused on these. What's more, some modification measures have been applied to improve the properties of LDH (e.g., noble metal modified LDHs and semiconductors/LDHs (G. Chen et al., 2019; C. Chen et al., 2019; C.R. Chen et al., 2019; Tonda and Jo, 2018; Seftel et al., 2015)), and whether these measures can be used to the modification of LDH-BC composites remains to be explored.

5. Conclusions and perspectives

This paper summarized the advances in LDH-BC composites from the synthetic methods, the application in adsorption and catalysis, and the underlying mechanisms, aiming at facilitating future research. By magnetic treatment, acid treatment, alkali treatment, controlling metal ion ratios, LDHs intercalation and calcination, LDH-BC composites with excellent physicochemical properties, showing good adsorption and catalytic effects, are designed and fabricated. LDH-BC composites will be more competitive in adsorption and catalysis by the modification of biochar and LDHs. However, there are still some directions of LDH-BC

composites need to be explored.

(1) Most of BC used in LDH-BC composites are prepared by conventional slow pyrolysis. Hydrochar prepared by hydrothermal carbonization has many advantages, such as low heating temperature (Meyer et al., 2011), less polluting gas in the pyrolysis process (Kang et al., 2012), a lower ash content, higher carbon retention, and more surface oxygen-containing groups (Kang et al., 2012; Liu et al., 2010). In addition, hydrothermal method can also be used to synthesize LDHs. Therefore, LDH-BC composites can be produced in "one-step" by hydrothermal carbonization of biomass in metal ion solution and urea solution. There are few studies about this synthesis process and application of LDH-hydrochar composites, more attention is needed. In addition to the synthesis of BC, mass ratio of LDHs to BC in synthesis and the metal ion leaching rate of LDH-BC composites during the reaction were merely studied. Therefore, more attention should be paid to these aspects to achieve better results in terms of removing contaminants.

(2) In adsorption mechanisms of Cr(VI), a study showed that Cr(VI) of CrO_4^{2-} could be reduced to Cr^{3+} by functional groups of LDH-BC composite which included C-C, C-O and C-N (Wang et al., 2020a). However, the specific reduction processes have not been explained. For example, how did the group of C-C affect the Cr (VI) reduction? or which type of C-C groups played the role in this process? What's more, as described in the article, the specific adsorption mechanisms of the removal of Pb(II) and Cd(II) are controversial. Therefore, more studies should be paid to these aspects.

(3) To date, most applications in adsorption on the performance of LDH-BC composites have mainly been carried out in the laboratory in a short-term ranging from several minutes to several hours. There are no field or pilot scale test yet. In addition, the stability and reusability of LDH-BC in real water matrices remains unknown. It is imperative to consider the long-term performance of LDH-BC before this technology is recommended for wastewater treatment.

(4) Recent AOP catalysis performance of LDH-BC composites has been mainly focused on removal efficiency of the target pollutants. However, the mineralization percent of the target pollutants as well as the toxicity of reaction intermediates in the AOPs are merely studied yet. Some of these intermediates in degradation processes are even more toxic than their parent compounds in some cases. Hence, more studies should be paid to this field to minimize the risks.

(5) Recently, the persulfate ion can be intercalated into LDHs by an ion exchange procedure. The activation of PDS only happened when the accommodation of 'guest' PDS into the interlayers of LDHs occurred. The reactivity of PDS can be enhanced by the basic sites on the LDHs laminate, which provide -OH to weaken the S–O bond of the PDS molecule and initiated the activation (Yang et al., 2020). In addition, the PDS-intercalated reduced graphene oxide (RGO)/LDH showed a better phenol catalytic performance than that of LDH-PDS counterpart. As the defective RGO sites activated the PDS on the surface or edges of LDHs layers, the breaking of the O-O bond in PDS generated $SO_4^{\cdot-}$ radicals from intercalated peroxydisulfate (Huang et al., 2020). It could be found that BC also have defective structure and oxygen-containing functional groups (e.g., -OH, -COOH), which can activate peroxydisulfate (B. Wang and Wang, 2020; X. Wang and Wang, 2020; S. Wang and Wang, 2020; Wu et al., 2018). Therefore, we deduce that PDS-intercalated LDH-BC composites may have a good degradation efficiency to organic pollutants. And more studies should focus on this aspect.

(6) At present, BC could be used the disinfection via visible light assisted heterogeneous photo-Fenton reaction or persulfate activation (Basu et al., 2021; Ho et al., 2019). And Lysozyme-LDH composites also showed excellent bactericidal effectiveness against *Staphylococcus aureus* (Yang et al., 2013). These applications belong to green disinfection technology and don't produce disinfection by-products. However, LDH-BC composites were mainly used to the degradation of pollutants in catalysis, and had no application in disinfection. Disinfection of LDH-BC composites via catalysis is worth exploring.

(7) Apart from the application in adsorption and catalysis, few studies have explored the applicability and efficiency of LDH-BC in agriculture. For example, P-loaded LDH-BC composites after adsorbing phosphate from wastewater could be recyclable as the slow-release fertilizer to promote growth of vegetation, or LDH-BC composite is used as a soil amendment preventing the leaching of soil nitrate. These indicate that LDH-BC composites have potential in agriculture. However, there are no further studies to verify and expand its effect in agriculture. Thus, innovative research should be focused on the development of agricultural applications, including the effect of different LDH-BC composites, stability under realistic conditions in agriculture, mechanisms in agriculture application.

(8) LDH-BC composites are mainly applied in the wastewater remediation. Although LDH-BC composites have a good removal efficiency on heavy metals and organics in wastewater treatment, LDH-BC composites have not been studied in the remediation of soil contaminated by heavy metals and organic pollutants. Therefore, new studies could explore the feasibility of LDH-BC composites in soil remediation.

Declaration of Competing Interest

The authors declare that they have no known competing financial interests or personal relationships that could have appeared to influence the work reported in this paper.

Acknowledgments

This research was financially supported by the National Key R&D Program of China (2020YFC1807600), the National Natural Science Foundation of China (51809089), and the Research and Development Plan of Key Areas in Hunan Province (2019NK2062).

References

Ahmad, M., Rajapaksha, A.U., Lim, J.E., Zhang, M., Bolan, N., Mohan, D., Vithanage, M., Lee, S.S., Ok, Y.S., 2014. Biochar as a sorbent for contaminant management in soil and water: a review. Chemosphere 99, 19–33.

Ai, L., Zhang, C., Meng, L., 2011. Adsorption of methyl orange from aqueous solution on hydrothermal synthesized Mg–Al layered double hydroxide. J. Chem. Eng. Data 56, 4217–4225.

Alagha, O., Manzar, M.S., Zubair, M., Anil, I., Mu'azu, N.D., Qureshi, A., 2020. Comparative adsorptive removal of phosphate and nitrate from wastewater using biochar-MgAl LDH nanocomposites: coexisting anions effect and mechanistic studies. Nanomaterials 10, 336.

Ashekuzzaman, S.M., Jiang, J.-Q., 2014. Study on the sorption–desorption–regeneration performance of Ca-, Mg- and CaMg-based layered double hydroxides for removing phosphate from water. Chem. Eng. J. 246, 97–105.

Azalok, K.A., Oladipo, A.A., Gazi, M., 2021a. UV-light-induced photocatalytic performance of reusable MnFe-LDO-biochar for tetracycline removal in water. J. Photochem. Photobiol. A Chem. 405, 112976.

Azalok, K.A., Oladipo, A.A., Gazi, M., 2021b. Hybrid MnFe-LDO-biochar nanopowders for degradation of metronidazole via UV-light-driven photocatalysis: Characterization and mechanism studies. Chemosphere 268, 128844.

Basu, A., Behera, M., Maharana, R., Kumar, M., Dhal, N.K., Tamhankar, A.J., Mishra, A., Lundborg, C.S., Tripathy, S.K., 2021. To unsnarl the mechanism of disinfection of Escherichia coli via visible light assisted heterogeneous photo-Fenton reaction in presence of biochar supported maghemite nanoparticles. J. Environ. Chem. Eng. 9, 104620.

Bolbol, H., Fekri, M., Hejazi-Mehrizi, M., 2019. Layered double hydroxide–loaded biochar as a sorbent for the removal of aquatic phosphorus: behavior and mechanism insights. Arab. J. Geosci. 12, 503.

Bukhtiyarova, M.V., 2019. A review on effect of synthesis conditions on the formation of layered double hydroxides. J. Solid State Chem. 269, 494–506.
Cai, P., Zheng, H., Wang, C., Ma, H.W., Hu, J.C., Pu, Y.B., Liang, P., 2012. Competitive adsorption characteristics of fluoride and phosphate on calcined Mg-Al-CO_3 layered double hydroxides. J. Hazard. Mater. 213, 100–108.
Cha, J.S., Park, S.H., Jung, S.-C., Ryu, C., Jeon, J.-K., Shin, M.-C., Park, Y.-K., 2016. Production and utilization of biochar: a review. J. Ind. Eng. Chem. 40, 1–15.
Chen, C., Zeng, H., Yi, M., Xiao, G., Xu, S., Shen, S., Feng, B., 2019. In-situ growth of Ag_3PO_4 on calcined Zn-Al layered double hydroxides for enhanced photocatalytic degradation of tetracycline under simulated solar light irradiation and toxicity assessment. Appl. Catal. B: Environ. 252, 47–54.
Chen, C.R., Zeng, H.Y., Yi, M.Y., Xiao, G.F., Zhu, R.L., Cao, X.J., Shen, S.G., Peng, J.W., 2019. Fabrication of Ag_2O/Ag decorated ZnAl-layered double hydroxide with enhanced visible light photocatalytic activity for tetracycline degradation. Ecotoxicol. Environ. Saf. 172, 423–431.
Chen, G., Zhang, X., Gao, Y., Zhu, G., Cheng, Q., Cheng, X., 2019. Novel magnetic MnO_2/$MnFe_2O_4$ nanocomposite as a heterogeneous catalyst for activation of peroxymonosulfate (PMS) toward oxidation of organic pollutants. Sep. Purif. Technol. 213, 456–464.
Chen, S., Xu, Z.P., Zhang, Q., Lu, G.Q.M., Hao, Z.P., Liu, S., 2009. Studies on adsorption of phenol and 4-nitrophenol on MgAl-mixed oxide derived from MgAl-layered double hydroxide. Sep. Purif. Technol. 67, 194–200.
Chen, W., Qu, B., 2004. LLDPE/ZnAl LDH-exfoliated nanocomposites: effects of nanolayers on thermal and mechanical properties. J. Mater. Chem. 14, 1705–1710.
Chen, X., Chen, G., Chen, L., Chen, Y., Lehmann, J., McBride, M.B., Hay, A.G., 2011. Adsorption of copper and zinc by biochars produced from pyrolysis of hardwood and corn straw in aqueous solution. Bioresour. Technol. 102, 8877–8884.
Cheng, X., Huang, X., Wang, X., Sun, D., 2010. Influence of calcination on the adsorptive removal of phosphate by Zn-Al layered double hydroxides from excess sludge liquor. J. Hazard. Mater. 177, 516–523.
Chetia, M., Goswamee, R.L., Banerjee, S., Chatterjee, S., Singh, L., Srivastava, R.B., Sarma, H.P., 2012. Arsenic removal from water using calcined Mg-Al layered double hydroxide. Clean Technol. Environ. Policy 14, 21–27.
Cui, Q., Jiao, G., Zheng, J., Wang, T., Wu, G., Li, G., 2019. Synthesis of a novel magnetic Caragana korshinskii biochar/Mg–Al layered double hydroxide composite and its strong adsorption of phosphate in aqueous solutions. RSC Adv. 9, 18641–18651.
Dai, S., Wang, N., Qi, C., Wang, X., Ma, Y., Yang, L., Liu, X., Huang, Q., Nie, C., Hu, B., Wang, X., 2019. Preparation of core-shell structure Fe_3O_4@C@MnO_2 nanoparticles for efficient elimination of U(VI) and Eu(III) ions. Sci. Total Environ. 685, 986–996.
Dong, X., Fu, J., Xiong, X., Chen, C., 2011. Preparation of hydrophilic mesoporous carbon and its application in dye adsorption. Mater. Lett. 65, 2486–2488.
dos Santos, G.E.D., Lins, P.V.D., Oliveira, L., da Silva, E.O., Anastopoulos, I., Erto, A., Giannakoudakis, D.A., de Almeida, A.R.F., Duarte, J.L.D., Meili, L., 2021. Layered double hydroxides/biochar composites as adsorbents for water remediation applications: recent trends and perspectives. J. Clean. Prod. 284, 124755.
Duan, Z., Zhang, W., Lu, M., Shao, Z., Huang, W., Li, J., Li, Y., Mo, J., Li, Y., Chen, C., 2020. Magnetic Fe_3O_4/activated carbon for combined adsorption and Fenton oxidation of 4-chlorophenol. Carbon 167, 351–363.
El Gaini, L., Lakraimi, M., Sebbar, E., Meghea, A., Bakasse, M., 2009. Removal of indigo carmine dye from water to Mg-Al-CO_3-calcined layered double hydroxides. J. Hazard Mater. 161, 627–632.
Fan, X., Cao, Q., Meng, F., Song, B., Bai, Z., Zhao, Y., Chen, D., Zhou, Y., Song, M., Fenton-like, A., 2021. A Fenton-like system of biochar loading Fe–Al layered double hydroxides (FeAl-LDH@BC) / H_2O_2 for phenol removal. Chemosphere 266, 128992.
Fan, Y., Wang, B., Yuan, S., Wu, X., Chen, J., Wang, L., 2010. Adsorptive removal of chloramphenicol from wastewater by NaOH modified bamboo charcoal. Bioresour. Technol. 101, 7661–7664.
Fang, G.D., Gao, J., Liu, C., Dionysiou, D.D., Wang, Y., Zhou, D.M., 2014. Key role of persistent free radicals in hydrogen peroxide activation by biochar: implications to organic contaminant degradation. Environ. Sci. Technol. 48, 1902–1910.
Fang, G.D., Zhu, C.Y., Dionysiou, D.D., Gao, J., Zhou, D.M., 2015. Mechanism of hydroxyl radical generation from biochar suspensions: implications to diethyl phthalate degradation. Bioresour. Technol. 176, 210–217.
Fu, Q.M., Tan, X.F., Ye, S.J., Ma, L.L., Gu, Y.L., Zhang, P., Chen, Q., Yang, Y.Y., Tang, Y. Q., 2021. Mechanism analysis of heavy metal lead captured by natural-aged microplastics. Chemosphere 270, 128624.
Geng, C., Xu, T., Li, Y., Chang, Z., Sun, X., Lei, X., 2013. Effect of synthesis method on selective adsorption of thiosulfate by calcined MgAl-layered double hydroxides. Chem. Eng. J. 232, 510–518.
Gholami, P., Khataee, A., Soltani, R.D.C., Dinpazhoh, L., Bhatnagar, A., 2020a. Photocatalytic degradation of gemifloxacin antibiotic using Zn-Co-LDH@biochar nanocomposite. J. Hazard Mater. 382, 121070.
Gholami, P., Dinpazhoh, L., Khataee, A., Hassani, A., Bhatnagar, A., 2020b. Facile hydrothermal synthesis of novel Fe-Cu layered double hydroxide/biochar nanocomposite with enhanced sonocatalytic activity for degradation of cefazolin sodium. J. Hazard. Mater. 381, 120742.
Goh, K.H., Lim, T.T., Dong, Z., 2008. Application of layered double hydroxides for removal of oxyanions: a review. Water Res 42, 1343–1368.
Goh, K.H., Lim, T.T., Dong, Z.L., 2009. Enhanced Arsenic removal by hydrothermally treated nanocrystalline Mg/Al layered double hydroxide with nitrate intercalation. Environ. Sci. Technol. 43, 2537–2543.
Golshan, M., Kakavandi, B., Ahmadi, M., Azizi, M., 2018. Photocatalytic activation of peroxymonosulfate by TiO_2 anchored on cupper ferrite (TiO_2@$CuFe_2O_4$) into 2,4-D degradation: process feasibility, mechanism and pathway. J. Hazard. Mater. 359, 325–337.
Han, H., Wei, W., Jiang, Z., Lu, J., Zhu, J., Xie, J., 2016. Removal of cationic dyes from aqueous solution by adsorption onto hydrophobic/hydrophilic silica aerogel. Colloids Surf. A Physicochem. Eng. Asp. 509, 539–549.
Ho, S.-H., Chen, Y.-d, Li, R., Zhang, C., Ge, Y., Cao, G., Ma, M., Duan, X., Wang, S., Ren, N.-q, 2019. N-doped graphitic biochars from C-phycocyanin extracted Spirulina residue for catalytic persulfate activation toward nonradical disinfection and organic oxidation. Water Res. 159, 77–86.
Huang, D., Liu, L., Zeng, G., Xu, P., Huang, C., Deng, L., Wang, R., Wan, J., 2017. The effects of rice straw biochar on indigenous microbial community and enzymes activity in heavy metal-contaminated sediment. Chemosphere 174, 545–553.
Huang, D., Liu, C., Zhang, C., Deng, R., Wang, R., Xue, W., Luo, H., Zeng, G., Zhang, Q., Guo, X., 2019. Cr(VI) removal from aqueous solution using biochar modified with Mg/Al-layered double hydroxide intercalated with ethylenediaminetetraacetic acid. Bioresour. Technol. 276, 127–132.
Huang, X., Su, Q., Han, S., Zhou, J., Qian, G., Gao, N., 2020. Efficient activation of intercalated persulfate via a composite of reduced graphene oxide and layered double hydroxide. J. Hazard. Mater. 389, 122051.
Huang, Z., Wang, T., Shen, M., Huang, Z., Chong, Y., Cui, L., 2019. Coagulation treatment of swine wastewater by the method of in-situ forming layered double hydroxides and sludge recycling for preparation of biochar composite catalyst. Chem. Eng. J. 369, 784–792.
Jia, Y., Zhang, Y., Fu, J., Yuan, L., Li, Z., Liu, C., Zhao, D., Wang, X., 2019. A novel magnetic biochar/MgFe-layered double hydroxides composite removing Pb^{2+} from aqueous solution: isotherms, kinetics and thermodynamics. Colloids Surf. A Physicochem. Eng. Asp. 567, 278–287.
Jiang, Y.H., Li, A.Y., Deng, H., Ye, C.H., Li, Y., 2019. Phosphate adsorption from wastewater using ZnAl-LDO-loaded modified banana straw biochar. Environ. Sci. Pollut. Res. Int. 26, 18343–18353.
Jin, H., Capareda, S., Chang, Z., Gao, J., Xu, Y., Zhang, J., 2014. Biochar pyrolytically produced from municipal solid wastes for aqueous As(V) removal: adsorption property and its improvement with KOH activation. Bioresour. Technol. 169, 622–629.
Jing, C., Dong, B., Zhang, Y., 2020. Chemical modifications of layered double hydroxides in the supercapacitor, energy & environmental. Materials 3, 346–379.
Kameda, T., Saito, S., Umetsu, Y., 2005. Mg-Al layered double hydroxide intercalated with ethylene-diaminetetraacetate anion: synthesis and application to the uptake of heavy metal ions from an aqueous solution. Sep. Purif. Technol. 47, 20–26.
Kameda, T., Takeuchi, H., Yoshioka, T., 2008. Uptake of heavy metal ions from aqueous solution using Mg-Al layered double hydroxides intercalated with citrate, malate, and tartrate. Sep. Purif. Technol. 62, 330–336.
Kang, S., Li, X., Fan, J., Chang, J., 2012. Characterization of hydrochars produced by hydrothermal carbonization of lignin, cellulose, d-xylose, and wood meal. Ind. Eng. Chem. Res. 51, 9023–9031.
Kappler, A., Wuestner, M.L., Ruecker, A., Harter, J., Halama, M., Behrens, S., 2014. Biochar as an electron shuttle between bacteria and Fe(III) minerals. Environ. Sci. Technol. Lett. 1, 339–344.
Khan, S.B., Alamry, K., Alyahyawi, N., Asiri, A., 2018. Controlled release of organic–inorganic nanohybrid: cefadroxil intercalated Zn–Al-layered double hydroxide. Int. J. Nanomed. Volume 13, 3203–3222.
Khataee, A., Arefi-Oskoui, S., Samaei, L., 2018a. ZnFe-Cl nanolayered double hydroxide as a novel catalyst for sonocatalytic degradation of an organic dye. Ultrason. Sonochem. 40, 703–713.
Khataee, A., Eghbali, P., Irani-Nezhad, M.H., Hassani, A., 2018b. Sonochemical synthesis of WS_2 nanosheets and its application in sonocatalytic removal of organic dyes from water solution. Ultrason. Sonochem. 48, 329–339.
Lan, M., Fan, G., Sun, W., Li, F., 2013. Synthesis of hybrid Zn–Al–In mixed metal oxides/carbon nanotubes composite and enhanced visible-light-induced photocatalytic performance. Appl. Surf. Sci. 282, 937–946.
Lee, S.Y., Choi, J.-W., Song, K.G., Choi, K., Lee, Y.J., Jung, K.-W., 2019. Adsorption and mechanistic study for phosphate removal by rice husk-derived biochar functionalized with Mg/Al-calcined layered double hydroxides via co-pyrolysis. Compos. Part B: Eng. 176, 107209.
Lehmann, J., Rillig, M.C., Thies, J., Masiello, C.A., Hockaday, W.C., Crowley, D., 2011. Biochar effects on soil biota – a review. Soil Biol. Biochem. 43, 1812–1836.
Lesbani, A., Asri, F., Palapa, N.R., Taher, T., Rachmat, A., 2020. Efficient removal of methylene blue by adsorption using composite based Ca/Al layered double hydroxide-biochar. Glob. Nest J. 22, 250–257.
Li, G.W., Huang, Z.J., Chen, C.Y., Cui, H.C., Su, Y.J., Yang, Y., Cui, L.H., 2019. Simultaneous adsorption of trace sulfamethoxazole and hexavalent chromium by biochar/MgAl layered double hydroxide composites. Environ. Chem. 16, 68–79.
Li, J., Fan, Q.H., Wu, Y.J., Wang, X.X., Chen, C.L., Tang, Z.Y., Wang, X.K., 2016. Magnetic polydopamine decorated with Mg-Al LDH nanoflakes as a novel bio-based adsorbent for simultaneous removal of potentially toxic metals and anionic dyes. J. Mater. Chem. A 4, 1737–1746.
Li, M., Liu, H., Chen, T., Dong, C., Sun, Y., 2019. Synthesis of magnetic biochar composites for enhanced uranium(VI) adsorption. Sci. Total Environ. 651, 1020–1028.
Li, R., Wang, J.J., Zhou, B., Awasthi, M.K., Ali, A., Zhang, Z., Gaston, L.A., Lahori, A.H., Mahar, A., 2016. Enhancing phosphate adsorption by Mg/Al layered double hydroxide functionalized biochar with different Mg/Al ratios. Sci. Total Environ. 559, 121–129.
Li, S.B., Dong, L.J., Wei, Z.F., Sheng, G.D., Du, K., Hu, B.W., 2020. Adsorption and mechanistic study of the invasive plant-derived biochar functionalized with CaAl-LDH for Eu(III) in water. J. Environ. Sci. 96, 127–137.

Li, S.T., Xu, H.M., Wang, L.L., Ji, L.P., Li, X.W., Qu, Z., Yan, N.Q., 2021. Dual-functional sites for selective adsorption of Mercury and Arsenic ions in $[SnS_4]^{4-}$/MgFe-LDH from wastewater. J. Hazard. Mater. 403, 123940.
Li, X., Wang, C., Zhang, J., Liu, J., Liu, B., Chen, G., 2020. Preparation and application of magnetic biochar in water treatment: a critical review. Sci. Total Environ. 711, 134847.
Lian, F., Cui, G., Liu, Z., Duo, L., Zhang, G., Xing, B., 2016. One-step synthesis of a novel N-doped microporous biochar derived from crop straws with high dye adsorption capacity. J. Environ. Manag. 176, 61–68.
Liu, H., Sun, X., Yin, C., Hu, C., 2008. Removal of phosphate by mesoporous ZrO_2. J. Hazard Mater. 151, 616–622.
Liu, H., Shan, J., Chen, Z., Lichtfouse, E., 2021. Efficient recovery of phosphate from simulated urine by Mg/Fe bimetallic oxide modified biochar as a potential resource. Sci. Total Environ. 784, 147546.
Liu, Y., Pang, H., Wang, X., Yu, S., Chen, Z., Zhang, P., Chen, L., Song, G., Alharbi, N.S., Rabah, S.O., Wang, X., 2021a. Zeolitic imidazolate framework-based nanomaterials for the capture of heavy metal ions and radionuclides: a review. Chem. Eng. J. 406, 127139.
Liu, Y., Huo, Y., Wang, X., Yu, S., Ai, Y., Chen, Z., Zhang, P., Chen, L., Song, G., Alharbi, N.S., Rabah, S.O., Wang, X., 2021b. Impact of metal ions and organic ligands on uranium removal properties by zeolitic imidazolate framework materials. J. Clean. Prod. 278, 123216.
Liu, Z., Zhang, F.-S., Wu, J., 2010. Characterization and application of chars produced from pinewood pyrolysis and hydrothermal treatment. Fuel 89, 510–514.
Luo, X., Huang, Z., Lin, J., Li, X., Qiu, J., Liu, J., Mao, X., 2020. Hydrothermal carbonization of sewage sludge and in-situ preparation of hydrochar/MgAl-layered double hydroxides composites for adsorption of Pb(II). J. Clean. Prod. 258, 120991.
Lv, Q., Wang, H.X., Zhang, M.L., Xue, J.B., Yang, J., 2020. Synthesis of magnetic biochar/carbonate intercalated Mg-Al layered double hydroxides for enhanced Cd (II) removal from aqueous solution. Desalin. Water Treat. 207, 258–269.
Lyu, H.H., Zhang, Q.R., Shen, B.X., 2020. Application of biochar and its composites in catalysis. Chemosphere 240, 124842.
Lyu, P., Wang, G., Wang, B., Yin, Q., Li, Y., Deng, N., 2021. Adsorption and interaction mechanism of uranium (VI) from aqueous solutions on phosphate-impregnation biochar cross-linked Mg Al layered double-hydroxide composite. Appl. Clay Sci. 209, 106146.
Meili, L., Lins, P.V., Zanta, C.L.P.S., Soletti, J.I., Ribeiro, L.M.O., Dornelas, C.B., Silva, T. L., Vieira, M.G.A., 2019. MgAl-LDH/Biochar composites for methylene blue removal by adsorption. Appl. Clay Sci. 168, 11–20.
Meyer, S., Glaser, B., Quicker, P., 2011. Technical, economical, and climate-related aspects of biochar production technologies: a literature review. Environ. Sci. Technol. 45, 9473–9483.
Mohan, D., Sarswat, A., Ok, Y.S., Pittman Jr., C.U., 2014. Organic and inorganic contaminants removal from water with biochar, a renewable, low cost and sustainable adsorbent—a critical review. Bioresour. Technol. 160, 191–202.
Mukherjee, A., Zimmerman, A.R., Harris, W., 2011. Surface chemistry variations among a series of laboratory-produced biochars. Geoderma 163, 247–255.
Mukome, F.N.D., Zhang, X., Silva, L.C.R., Six, J., Parikh, S.J., 2013. Use of chemical and physical characteristics to investigate trends in biochar feedstocks. J. Agric. Food Chem. 61, 2196–2204.
Nakayama, H., Hirami, S., Tsuhako, M., 2007. Selective adsorption of mercury ion by mercaptocarboxylic acid intercalated Mg-Al layered double hydroxide. J. Colloid Interface Sci. 315, 177–183.
Nguyen, T.T.N., Xu, C.-Y., Tahmasbian, I., Che, R., Xu, Z., Zhou, X., Wallace, H.M., Bai, S. H., 2017. Effects of biochar on soil available inorganic nitrogen: a review and meta-analysis. Geoderma 288, 79–96.
Oestreicher, V., Jobbágy, M., Regazzoni, A.E., 2014. Halide exchange on Mg(II)–Al(III) layered double hydroxides: exploring affinities and electrostatic predictive models. Langmuir 30, 8408–8415.
Pang, H.W., Huang, S.Y., Wu, Y.H., Yang, D.X., Wang, X.X., Yu, S.J., Chen, Z.S., Alsaedi, A., Hayat, T., Wang, X.K., 2018. Efficient elimination of U(VI) by polyethyleneimine-decorated fly ash. Inorg. Chem. Front. 5, 2399–2407.
Pavlovic, I., Perez, M.R., Barriga, C., Ulibarri, M.A., 2009. Adsorption of Cu^{2+}, Cd^{2+} and Pb^{2+} ions by layered double hydroxides intercalated with the chelating agents diethylenetriaminepentaacetate and meso-2,3-dimercaptosuccinate. Appl. Clay Sci. 43, 125–129.
Peng, Y.T., Sun, Y.Q., Hanif, A., Shang, J., Shen, Z.T., Hou, D.Y., Zhou, Y.Y., Chen, Q., Ok, Y.S., Tsang, D.C.W., 2021. Design and fabrication of exfoliated Mg/Al layered double hydroxides on biochar support. J. Clean. Prod. 289, 125142.
Qin, F., Peng, Y., Song, G., Fang, Q., Wang, R., Zhang, C., Zeng, G., Huang, D., Lai, C., Zhou, Y., Tan, X., Cheng, M., Liu, S., 2020. Degradation of sulfamethazine by biochar-supported bimetallic oxide/persulfate system in natural water: Performance and reaction mechanism. J. Hazard. Mater. 398, 122816.
Qin, H., Cheng, H., Li, H., Wang, Y., 2020. Degradation of ofloxacin, amoxicillin and tetracycline antibiotics using magnetic core–shell $MnFe_2O_4$@C-NH_2 as a heterogeneous Fenton catalyst. Chem. Eng. J. 396, 125304.
Qin, J., Niu, A., Li, Q., Liu, Y., Lin, C., 2020. Effect of soluble calcium on enhancing nitrate retention by biochar. J. Environ. Manag. 274, 111133.
Qiu, M., Liu, Z., Wang, S., Hu, B., 2021. The photocatalytic reduction of U(VI) into U(IV) by ZIF-8/g-C_3N_4 composites at visible light. Environ. Res. 196, 110349.
Rahman, S., Navarathna, C.M., Das, N.K., Alchouron, J., Reneau, P., Stokes, S., Thirumalai, R.V.K.G., Perez, F., Hassan, E.B., Mohan, D., Pittman Jr., C.U., Mlsna, T., 2021. High capacity aqueous phosphate reclamation using Fe/Mg-layered double hydroxide (LDH) dispersed on biochar. J. Colloid Interface Sci. 597, 182–195.
Rojas, R., Perez, M.R., Erro, E.M., Ortiz, P.I., Ulibarri, M.A., Giacomelli, C.E., 2009. EDTA modified LDHs as Cu^{2+} scavengers: removal kinetics and sorbent stability. J. Colloid Interface Sci. 331, 425–431.
Seftel, E.M., Niarchos, M., Mitropoulos, C., Mertens, M., Vansant, E.F., Cool, P., 2015. Photocatalytic removal of phenol and methylene-blue in aqueous media using TiO_2@LDH clay nanocomposites. Catal. Today 252, 120–127.
Shafiq, M., Alazba, A.A., Amin, M.T., 2020. Adsorption of divalent copper ions from synthetic wastewater using layered double hydroxides (NiZnFe) and its composites with banana biochar and carbon nanotubes. Water Air Soil Pollut. 231, 346.
Shafiq, M., Alazba, A.A., Amin, M.T., 2021. Application of Zn-Fe layered double hydroxide and its composites with biochar and carbon nanotubes to the adsorption of lead in a batch system: kinetics and isotherms. Arab. J. Sci. Eng. 21, 05576.
Shan, C., Ma, Z., Tong, M., 2014. Efficient removal of trace antimony(III) through adsorption by hematite modified magnetic nanoparticles. J. Hazard. Mater. 268, 229–236.
Shan, R.-r., Yan, L.-g., Yang, K., Yu, S.-j., Hao, Y.-f., Yu, H.-q., Du, B., 2014. Magnetic Fe_3O_4/MgAl-LDH composite for effective removal of three red dyes from aqueous solution. Chem. Eng. J. 252, 38–46.
Shao, H., Zhao, X., Wang, Y., Mao, R., Wang, Y., Qiao, M., Zhao, S., Zhu, Y., 2017. Synergetic activation of peroxymonosulfate by Co_3O_4 modified g-C_3N_4 for enhanced degradation of diclofenac sodium under visible light irradiation. Appl. Catal. B-Environ. 218, 810–818.
Son, E.-B., Poo, K.-M., Chang, J.-S., Chae, K.-J., 2018. Heavy metal removal from aqueous solutions using engineered magnetic biochars derived from waste marine macro-algal biomass. Sci. Total Environ. 615, 161–168.
de Souza dos Santos, G.E., Ide, A.H., Duarte, J.L.S., McKay, G., Silva, A.O.S., Meili, L., 2020. Adsorption of anti-inflammatory drug diclofenac by MgAl/layered double hydroxide supported on Syagrus coronata biochar. Powder Technol. 364, 229–240.
Su, J.F., Bai, Y.H., Huang, T.L., Gao, Y.C., Wei, L., Lu, J.S., 2019. Performance and microbial community of simultaneous denitrification and biomineralization in bioreactors. Chem. Eng. Technol. 42, 637–644.
Sun, Y., Gao, B., Yao, Y., Fang, J., Zhang, M., Zhou, Y., Chen, H., Yang, L., 2014. Effects of feedstock type, production method, and pyrolysis temperature on biochar and hydrochar properties. Chem. Eng. J. 240, 574–578.
Tan, X., Liu, Y., Zeng, G., Wang, X., Hu, X., Gu, Y., Yang, Z., 2015. Application of biochar for the removal of pollutants from aqueous solutions. Chemosphere 125, 70–85.
Tan, X., Liu, S., Liu, Y., Gu, Y., Zeng, G., Cai, X., Yan, Z., Yang, C., Hu, X., Chen, B., 2016. One-pot synthesis of carbon supported calcined-Mg/Al layered double hydroxides for antibiotic removal by slow pyrolysis of biomass waste. Sci. Rep. 6, 39691.
Tan, X.F., Liu, Y.G., Gu, Y.L., Liu, S.B., Zeng, G.M., Cai, X., Hu, X.J., Wang, H., Liu, S.M., Jiang, L.H., 2016. Biochar pyrolyzed from MgAl-layered double hydroxides pre-coated ramie biomass (Boehmeria nivea (L.) Gaud.): Characterization and application for crystal violet removal. J. Environ. Manag. 184, 85–93.
Tan, Y., Yin, X., Wang, C., Sun, H., Ma, A., Zhang, G., Wang, N., 2019. Sorption of cadmium onto Mg-Fe layered double hydroxide (LDH)-Kiwi branch biochar. Environ. Pollut. Bioavailab. 31, 189–197.
Tan, Z., Yuan, S., Hong, M., Zhang, L., Huang, Q., 2020. Mechanism of negative surface charge formation on biochar and its effect on the fixation of soil Cd. J. Hazard. Mater. 384, 121370.
Tezuka, S., Chitrakar, R., Sonoda, A., Ooi, K., Tomida, T., 2004. Studies on selective adsorbents for oxo-anions. Nitrate ion-exchange properties of layered double hydroxides with different metal atoms. Green. Chem. 6, 104–109.
Thines, K.R., Abdullah, E.C., Mubarak, N.M., Ruthiraan, M., 2017. Synthesis of magnetic biochar from agricultural waste biomass to enhancing route for waste water and polymer application: a review. Renew. Sustain. Energy Rev. 67, 257–276.
Tonda, S., Jo, W.-K., 2018. Plasmonic Ag nanoparticles decorated NiAl-layered double hydroxide/graphitic carbon nitride nanocomposites for efficient visible-light-driven photocatalytic removal of aqueous organic pollutants. Catal. Today 315, 213–222.
Valletregi, M., 2004. Hexagonal ordered mesoporous material as a matrix for the controlled release of amoxicillin. Solid State Ion. 172, 435–439.
Vithanage, M., Ashiq, A., Ramanayaka, S., Bhatnagar, A., 2020. Implications of layered double hydroxides assembled biochar composite in adsorptive removal of contaminants: current status and future perspectives. Sci. Total Environ. 737, 139718.
Wan, D., Liu, H., Liu, R., Qu, J., Li, S., Zhang, J., 2012. Adsorption of nitrate and nitrite from aqueous solution onto calcined (Mg–Al) hydrotalcite of different Mg/Al ratio. Chem. Eng. J., 195- 196, 241–247.
Wan, S., Wang, S., Li, Y., Gao, B., 2017. Functionalizing biochar with Mg–Al and Mg–Fe layered double hydroxides for removal of phosphate from aqueous solutions. J. Ind. Eng. Chem. 47, 246–253.
Wang, B., Li, Y., Zheng, J., Hu, Y., Wang, X., Hu, B., 2020. Efficient removal of U(VI) from aqueous solutions using the magnetic biochar derived from the biomass of a bloom-forming cyanobacterium (Microcystis aeruginosa). Chemosphere 254, 126898.
Wang, C., Wang, H., 2018. Pb(II) sorption from aqueous solution by novel biochar loaded with nano-particles. Chemosphere 192, 1–4.
Wang, H., Wang, S., Chen, Z., Zhou, X., Wang, J., Chen, Z., 2020a. Engineered biochar with anisotropic layered double hydroxide nanosheets to simultaneously and efficiently capture Pb^{2+} and CrO_4^{2-} from electroplating wastewater. Bioresour. Technol. 306, 123118.
Wang, H., Zhao, W., Chen, Y., Li, Y., 2020b. Nickel aluminum layered double oxides modified magnetic biochar from waste corncob for efficient removal of acridine orange. Bioresour. Technol. 315, 123834.
Wang, J., Wang, S., 2019. Preparation, modification and environmental application of biochar: a review. J. Clean. Prod. 227, 1002–1022.

Wang, M., Wang, J.J., Tafti, N.D., Hollier, C.A., Myers, G., Wang, X., 2019. Effect of alkali-enhanced biochar on silicon uptake and suppression of gray leaf spot development in perennial ryegrass. Crop Prot. 119, 9–16.
Wang, S., Wang, J., 2020. Kinetics of PMS activation by graphene oxide and biochar. Chemosphere 239, 124812.
Wang, S., Gao, B., Zimmerman, A.R., Li, Y., Ma, L., Harris, W.G., Migliaccio, K.W., 2015. Removal of arsenic by magnetic biochar prepared from pinewood and natural hematite. Bioresour. Technol. 175, 391–395.
Wang, S., Gao, B., Li, Y., Zimmerman, A.R., Cao, X., 2016a. Sorption of arsenic onto Ni/Fe layered double hydroxide (LDH)-biochar composites. RSC Adv. 6, 17792–17799.
Wang, S., Gao, B., Li, Y., 2016b. Enhanced arsenic removal by biochar modified with nickel (Ni) and manganese (Mn) oxyhydroxides. J. Ind. Eng. Chem. 37, 361–365.
Wang, T., Li, C., Wang, C., Wang, H., 2018. Biochar/MnAl-LDH composites for Cu (II) removal from aqueous solution. Colloids Surf. A Physicochem. Eng. Asp. 538, 443–450.
Wang, T., Zhang, D., Fang, K., Zhu, W., Peng, Q., Xie, Z., 2021. Enhanced nitrate removal by physical activation and Mg/Al layered double hydroxide modified biochar derived from wood waste: adsorption characteristics and mechanisms. J. Environ. Chem. Eng. 9, 105184.
Wang, X., Jin, H., Wu, D., Nie, Y., Tian, X., Yang, C., Zhou, Z., Li, Y., 2020. Fe_3O_4@S-doped ZnO: a magnetic, recoverable, and reusable Fenton-like catalyst for efficient degradation of ofloxacin under alkaline conditions. Environ. Res. 186, 109626.
Wang, X.H., Gu, Y.L., Tan, X.F., Liu, Y.G., Zhou, Y.H., Hu, X.J., Cai, X.X., Xu, W.H., Zhang, C., Liu, S.H., 2019. Functionalized biochar/clay composites for reducing the bioavailable fraction of Arsenic and Cadmium in River Sediment. Environ. Toxicol. Chem. 38, 2337–2347.
Wang, Y., Zhao, X., Cao, D., Wang, Y., Zhu, Y., 2017. Peroxymonosulfate enhanced visible light photocatalytic degradation bisphenol A by single-atom dispersed Ag mesoporous g-C_3N_4 hybrid. Appl. Catal. B-Environ. 211, 79–88.
Wang, Y., Yan, D., El Hankari, S., Zou, Y., Wang, S., 2018. Recent progress on layered double hydroxides and their derivatives for electrocatalytic water splitting. Adv. Sci. 5, 1800064.
Wu, M.J., Wu, J.Z., Zhang, J., Chen, H., Zhou, J.Z., Qian, G.R., Xu, Z.P., Du, Z., Rao, Q.L., 2018. A review on fabricating heterostructures from layered double hydroxides for enhanced photocatalytic activities. Catal. Sci. Technol. 8, 1207–1228.
Wu, Y., Guo, J., Han, Y., Zhu, J., Zhou, L., Lan, Y., 2018. Insights into the mechanism of persulfate activated by rice straw biochar for the degradation of aniline. Chemosphere 200, 373–379.
Xiao, B., Dai, Q., Yu, X., Yu, P., Zhai, S., Liu, R., Guo, X., Liu, J., Chen, H., 2018. Effects of sludge thermal-alkaline pretreatment on cationic red X-GRL adsorption onto pyrolysis biochar of sewage sludge. J. Hazard. Mater. 343, 347–355.
Xiao, Z., Zhang, L., Wu, L., Chen, D., 2019. Adsorptive removal of Cu(II) from aqueous solutions using a novel macroporous bead adsorbent based on poly(vinyl alcohol)/sodium alginate/$KMnO_4$ modified biochar. J. Taiwan Inst. Chem. Eng. 102, 110–117.
Xue, L., Gao, B., Wan, Y., Fang, J., Wang, S., Li, Y., Muñoz-Carpena, R., Yang, L., 2016. High efficiency and selectivity of MgFe-LDH modified wheat-straw biochar in the removal of nitrate from aqueous solutions. J. Taiwan Inst. Chem. Eng. 63, 312–317.
Yang, F., Zhang, S., Sun, Y., Tsang, D.C.W., Cheng, K., Ok, Y.S., 2019. Assembling biochar with various layered double hydroxides for enhancement of phosphorus recovery. J. Hazard Mater. 365, 665–673.
Yang, K., Yang, Z., Zhang, C., Gu, Y., Wei, J., Li, Z., Ma, C., Yang, X., Song, K., Li, Y., Fang, Q., Zhou, J., 2021a. Recent advances in CdS-based photocatalysts for CO_2 photocatalytic conversion. Chem. Eng. J. 418, 129344.
Yang, Q., Cui, P., Liu, C., Fang, G., Huang, M., Wang, Q., Zhou, Y., Hou, H., Wang, Y., 2021. In situ stabilization of the adsorbed Co^{2+} and Ni^{2+} in rice straw biochar based on LDH and its reutilization in the activation of peroxymonosulfate. J. Hazard. Mater. 416, 126215.
Yang, Z., Zhang, C., Zeng, G., Tan, X., Huang, D., Zhou, J., Fang, Q, Yang, K., Wang, H., Wei, J., Nie, K., 2021. State-of-the-art progress in the rational design of layered double hydroxide based photocatalysts for photocatalytic and photoelectrochemical H_2/O_2 production. Coord. Chem. Rev. 446, 214103.
Yang, Q.Z., Chang, Y.Y., Zhao, H.Z., 2013. Preparation and antibacterial activity of lysozyme and layered double hydroxide nanocomposites. Water Res. 47, 6712–6718.
Yang, X., Xu, G., Yu, H., Zhang, Z., 2016. Preparation of ferric-activated sludge-based adsorbent from biological sludge for tetracycline removal. Bioresour. Technol. 211, 566–573.
Yang, Z., Wang, F., Zhang, C., Zeng, G., Tan, X., Yu, Z., Zhong, Y., Wang, H., Cui, F., 2016. Utilization of LDH-based materials as potential adsorbents and photocatalysts for the decontamination of dyes wastewater: a review. RSC Adv. 6, 79415–79436.
Yang, Z.-z, Zhang, C., Zeng, G.-m, Tan, X.-f, Wang, H., Huang, D.-l, Yang, K.-h, Wei, J.-j, Ma, C., Nie, K., 2020. Design and engineering of layered double hydroxide based catalysts for water depollution by advanced oxidation processes: a review. J. Mater. Chem. A 8, 4141–4173.
Yap, M.W., Mubarak, N.M., Sahu, J.N., Abdullah, E.C., 2017. Microwave induced synthesis of magnetic biochar from agricultural biomass for removal of lead and cadmium from wastewater. J. Ind. Eng. Chem. 45, 287–295.
Ye, Q., Wu, J., Wu, P., Rehman, S., Ahmed, Z., Zhu, N., 2021. Enhancing peroxymonosulfate activation by Co-Fe layered double hydroxide catalysts via compositing with biochar. Chem. Eng. J. 417, 129111.
Ye, S., Cheng, M., Zeng, G., Tan, X., Wu, H., Liang, J., Shen, M., Song, B., Liu, J., Yang, H., Zhang, Y., 2020. Insights into catalytic removal and separation of attached metals from natural-aged microplastics by magnetic biochar activating oxidation process. Water Res. 179, 115876.
Yi, Y., Tu, G., Zhao, D., Tsang, P.E., Fang, Z., 2019. Biomass waste components significantly influence the removal of Cr(VI) using magnetic biochar derived from four types of feedstocks and steel pickling waste liquor. Chem. Eng. J. 360, 212–220.
Yi, Y., Huang, Z., Lu, B., Xian, J., Tsang, E.P., Cheng, W., Fang, J., Fang, Z., 2020. Magnetic biochar for environmental remediation: a review. Bioresour. Technol. 298, 122468.
Yu, S., Wang, X., Chen, Z., Wang, J., Wang, S., Hayat, T., Wang, X., 2017. Layered double hydroxide intercalated with aromatic acid anions for the efficient capture of aniline from aqueous solution. J. Hazard Mater. 321, 111–120.
Zhang, B., Dong, Z., Sun, D., Wu, T., Li, Y., 2017. Enhanced adsorption capacity of dyes by surfactant-modified layered double hydroxides from aqueous solution. J. Ind. Eng. Chem. 49, 208–218.
Zhang, C., Gao, Y., Yan, Q., Wang, Q., 2020. Fundamental investigation on layered double hydroxides derived mixed metal oxides for selective catalytic reduction of NOx by H_2. Catal. Today 355, 450–457.
Zhang, H., Xue, G., Chen, H., Li, X., 2018. Magnetic biochar catalyst derived from biological sludge and ferric sludge using hydrothermal carbonization: preparation, characterization and its circulation in Fenton process for dyeing wastewater treatment. Chemosphere 191, 64–71.
Zhang, J., Hu, H., Li, Z., Lou, X.W.D., 2016. Double-shelled nanocages with cobalt hydroxide inner shell and layered double hydroxides outer shell as high-efficiency polysulfide mediator for lithium-sulfur batteries. Angew. Chem. Int. Ed. 55, 3982–3986.
Zhang, L., Tang, S., Jiang, C., Jiang, X., Guan, Y., 2018. Simultaneous and efficient capture of inorganic nitrogen and heavy metals by polyporous layered double hydroxide and biochar composite for agricultural nonpoint pollution control. ACS Appl. Mater. Interfaces 10, 43013–43030.
Zhang, M., Gao, B., Yao, Y., Inyang, M., 2013. Phosphate removal ability of biochar/MgAl-LDH ultra-fine composites prepared by liquid-phase deposition. Chemosphere 92, 1042–1047.
Zhang, M., Gao, B., Fang, J., Creamer, A.E., Ullman, J.L., 2014. Self-assembly of needle-like layered double hydroxide (LDH) nanocrystals on hydrochar: characterization and phosphate removal ability. RSC Adv. 4, 28171–28175.
Zhang, M., Song, G., Gelardi, D.L., Huang, L., Khan, E., Mašek, O., Parikh, S.J., 2020. Evaluating biochar and its modifications for the removal of ammonium, nitrate, and phosphate in water. Water Res. 186, 116303.
Zhang, T., Yue, X., Gao, L., Qiu, F., Xu, J., Rong, J., Pan, J., 2017. Hierarchically porous bismuth oxide/layered double hydroxide composites: Preparation, characterization and iodine adsorption. J. Clean. Prod. 144, 220–227.
Zhang, W., Liu, Y.G., Tan, X.F., Zeng, G.M., Gong, J.L., Lai, C., Niu, Q.Y., Tang, Y.Q., 2019. Enhancement of detoxification of petroleum hydrocarbons and heavy metals in oil-contaminated soil by using glycine-β-cyclodextrin. IJERPH 16, 1155.
Zhang, W., Tan, X.F., Gu, Y.L., Liu, S.B., Liu, Y.G., Hu, X.J., Li, J., Zhou, Y.H., Liu, S.J., He, Y., 2020. Rice waste biochars produced at different pyrolysis temperatures for arsenic and cadmium abatement and detoxification in sediment. Chemosphere 250, 126268.
Zhang, Z., Yan, L., Yu, H., Yan, T., Li, X., 2019. Adsorption of phosphate from aqueous solution by vegetable biochar/layered double oxides: fast removal and mechanistic studies. Bioresour. Technol. 284, 65–71.
Zhao, D., Sheng, G., Hu, J., Chen, C., Wang, X., 2011. The adsorption of Pb(II) on Mg_2Al layered double hydroxide. Chem. Eng. J. 171, 167–174.
Zhao, H., Lang, Y., 2018. Adsorption behaviors and mechanisms of florfenicol by magnetic functionalized biochar and reed biochar. J. Taiwan Inst. Chem. Eng. 88, 152–160.
Zheng, Z., Ali, A., Su, J., Fan, Y., Zhang, S., 2021. Layered double hydroxide modified biochar combined with sodium alginate: A powerful biomaterial for enhancing bioreactor performance to remove nitrate. Bioresour. Technol. 323, 124630.
Zhong, X., Lu, Z., Liang, W., Guo, X., Hu, B., 2020. The fabrication of 3D hierarchical flower-like δ-MnO_2@COF nanocomposites for the efficient and ultra-fast removal of UO_2^{2+} ions from aqueous solution. Environ. Sci.: Nano 7, 3303–3317.
Zhu, M.X., Li, Y.P., Xie, M., Xin, H.Z., 2005. Sorption of an anionic dye by uncalcined and calcined layered double hydroxides: a case study. J. Hazard Mater. 120, 163–171.
Zhu, Y., Zhu, R., Xi, Y., Zhu, J., Zhu, G., He, H., 2019. Strategies for enhancing the heterogeneous Fenton catalytic reactivity: a review. Appl. Catal. B: Environ. 255, 117739.
Zoroufchi Benis, K., Motalebi Damuchali, A., Soltan, J., McPhedran, K.N., 2020. Treatment of aqueous arsenic – a review of biochar modification methods. Sci. Total Environ. 739, 139750.
Zubair, M., Manzar, M.S., Mu'azu, N.D., Anil, I., Blaisi, N.I., Al-Harthi, M.A., 2020. Functionalized MgAl-layered hydroxide intercalated date-palm biochar for enhanced uptake of cationic dye: kinetics, isotherm and thermodynamic studies. Appl. Clay Sci. 190, 105587.
Zubair, M., Ihsanullah, I., Aziz, H.A., Ahmad, M.A., Al-Harthi, M.A., 2021a. Sustainable wastewater treatment by biochar/layered double hydroxide composites: progress, challenges, and outlook. Bioresour. Technol. 319, 124128.
Zubair, M., Aziz, H.A., Ihsanullah, I., Ahmad, M.A., Al-Harthi, M.A., 2021b. Biochar supported CuFe layered double hydroxide composite as a sustainable adsorbent for efficient removal of anionic azo dye from water. Environ. Technol. Innov. 23, 101614.